

**OPEN ACCESS**

## Review—Non-Invasive Monitoring of Human Health by Exhaled Breath Analysis: A Comprehensive Review

To cite this article: Sagnik Das and Mrinal Pal 2020 *J. Electrochem. Soc.* **167** 037562

View the [article online](#) for updates and enhancements.



# Review—Non-Invasive Monitoring of Human Health by Exhaled Breath Analysis: A Comprehensive Review

Sagnik Das and Mrinal Pal<sup>z</sup>

Functional Materials and Devices Division, CSIR-Central Glass & Ceramic Research Institute, Jadavpur, Kolkata-700 032, India

Exhaled human breath analysis is a very promising field of research work having great potential for diagnosis of diseases in non-invasive way. Breath analysis has attracted huge attention in the field of medical diagnosis and disease monitoring in the last two decades. VOCs/gases (Volatile Organic Compounds) in exhaled breath bear the finger-prints of metabolic and biophysical processes going on in human body. It's a non-invasive, fast, non-hazardous, cost effective, and point of care process for disease state monitoring and environmental exposure assessment in human beings. Some VOCs/gases in exhaled breath are bio-markers of different diseases and their presence in excess amount is indicative of un-healthiness. Breath analysis has the potential for early detection of diseases. However, it is still underused and commercial device is yet not available owing to multifarious challenges. This review is intended to provide an overview of major biomarkers (VOCs/gases) present in exhaled breath, importance of their analysis towards disease monitoring, analytical techniques involved, promising materials for breath analysis etc. Finally, related challenges and limitations along with future scope will be touched upon.

© 2020 The Author(s). Published on behalf of The Electrochemical Society by IOP Publishing Limited. This is an open access article distributed under the terms of the Creative Commons Attribution 4.0 License (CC BY, <http://creativecommons.org/licenses/by/4.0/>), which permits unrestricted reuse of the work in any medium, provided the original work is properly cited. [DOI: 10.1149/1945-7111/ab67a6]



Manuscript submitted September 17, 2019; revised manuscript received December 2, 2019. Published February 3, 2020. *This paper is part of the JES Focus Issue on Sensor Reviews.*

Exhaled breath analysis an important area of research work which has gained tremendous interest recently owing to the advances in analytical techniques and nanotechnology. This is a non-invasive method for disease detection, therapeutic monitoring, and metabolic status monitoring by analyzing the volatile organic compounds (VOCs) present in the exhaled breath. Along with point of care detection breath analysis has the advantage of non-invasive, cost-effective, real time, qualitative/quantitative disease diagnosis<sup>1–3</sup> and hence it has the potential of replacing traditional blood test which is invasive and pain-staking. Alongside exhaled breath VOCs are also emitted from urine, sputum and faces<sup>1</sup> (all non-invasive in nature) also but breath is easiest of all these to handle and hence has the obvious edge over the other clinical sample.

Exhaled breath analysis for disease diagnosis is an ancient practice: even in the time of Hippocrates this was in vogue. Sweet breath odor was linked with diabetes and fish-like smell in exhaled breath was identified with kidney-related diseases.<sup>4</sup> In the late 1780s Lavoisier took the first initiative to determine the chemical components of human breath. In 1971 Linus Pauling demonstrated that breath is a complex gas containing no less than 200 VOCs and this for sure marked the beginning of the modern breath testing.<sup>5</sup> Later, Michael Phillips demonstrated that breath contains more than 300 VOCs.<sup>6</sup> Now it is known that breath contains more than 3500 VOCs.<sup>7</sup>

Human exhaled breath mostly contains, nitrogen (78.04%), oxygen [16%], carbon dioxide [4%–5%], hydrogen [5%],<sup>8</sup> inert gases [0.9%]<sup>9</sup> and water vapor. Other than that, it contains inorganics VOCs viz. nitric oxide (10–50 ppb),<sup>10</sup> nitrous oxide (1–20 ppb),<sup>10</sup> ammonia (0.5–2 ppm),<sup>11</sup> carbon monoxide (0–6 ppm),<sup>9</sup> hydrogen sulphide (0–1.3 ppm)<sup>12</sup> etc. and organic VOCs such as acetone (0.3–1 ppm),<sup>13</sup> ethanol, isoprene (~105 ppb),<sup>14</sup> ethane (0–10 ppb), methane (2–10 ppm), pentane [0–10 ppb]<sup>10</sup> etc. The air that is inhaled goes into the alveoli in the lungs where the metabolic excretable products diffuse into the inhaled air and then it is rejected in the form of exhaled air. Therefore, the exhaled air must carry the fingerprint of the metabolic process going on endogenously. Hence it is a rich source for disease diagnosis and health monitoring. As such the principle of breath analysis is thus simple. However, it is fraught with challenges that makes it complex. Firstly, a healthy human being exhales around 500 ml of breath out of which 150 ml is dead

space air which comes from the upper air tract; this does not exchange VOC/gas with the blood and therefore acts as a diluent only.<sup>15,16</sup> Secondly, many of the exhaled breath VOCs/gases are partially or fully of exogenous in origin<sup>17,18</sup> and depends on ambient air concentration, duration of exposure, solubility and partition coefficient, mass and fat content of the individual etc. Thirdly, non-volatile components such as isopropanes, peroxyinitrite etc, present as aerosol in breath can be measured only from breath condensate.<sup>19</sup> Fourthly, oral hygiene is a problem for many people. Finally, it is very difficult to detect a particular VOC with very low concentration (ppm/ppb) among thousand others. In addition, age, gender, food habit and pregnancy in case of women affects the breath composition.<sup>20–24</sup> Furthermore, there are no standards for breath collection techniques. In spite of all these challenges breath analysis is much easier than blood testing and therefore has attracted the attention of researchers in recent times.

In this review we will discuss the different techniques for the detection of breath biomarkers with a focus on semiconducting materials and their mechanism of gas sensing. It is in this context that we will also discuss the metabolic pathways for the generation of different breath biomarkers and their connection with different diseases; breath collection, preconcentration, desorption and storage; nanomaterials and sensor arrays for the detection of different cancers and finally the potential and plausible future of breath research. Indeed, there are multiple reviews in this topic but one must understand that this is a rapidly growing field of research. Righettoni et al.<sup>25</sup> reported that since the year 2000, ~140000 research papers have been published only on the topic of breath analysis itself. Therefore, comprehensive reviews must come up every year so as to keep the researchers around the globe informed about the recent progresses in the field.

## Diseases and Disorders Indicated by Important Biomarkers

The most important biomarkers of diseases in human body are ammonia, acetone, isoprene, nitic oxide, hydrogen sulphide, methane, ethane and pentane. In this section we will discuss the metabolic pathways of removal of these biomarkers and also will delineate in short, the diseases indicated by those when excreted in less or excess amount through the exhaled breath.

**Ammonia (NH<sub>3</sub>).**—Ammonia has essential nutritional values for human body, viz. synthesis of purines and pyrimidines, amino sugar

<sup>z</sup>E-mail: palm@cgcir.res.in

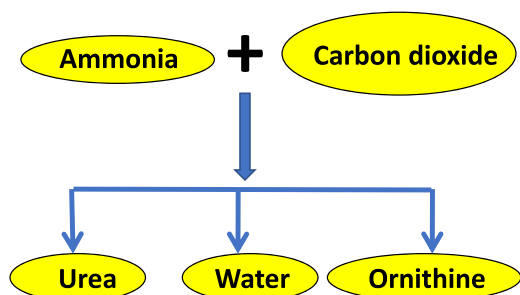


**Figure 1.** Elimination of excess ammonia from human body in the form of urea.

synthesis, maintaining the acid-base balance in the blood and producing non-essential amino acids in the body. However, excess ammonia in the body acts as toxin. Therefore, excess ammonia is removed from the body by urea cycle or ornithine cycle that converts ammonia into urea which is excreted in the form of urine through kidney. Figure 1, briefly shows the urea cycle.<sup>26–28</sup> This cycle takes place in liver and kidney. Therefore, if there is a problem in the liver or renal functioning it is reflected in an increased concentration of ammonia in exhaled breath, as a part of it is also excreted through breath.

Increased breath ammonia indicates several diseases, viz. kidney failure, liver dysfunction,<sup>29</sup> hepatic encephalopathy, swelling of brain, type-II Alzheimer's disease<sup>30</sup> etc. Increased ammonia in exhaled breath may also indicate peptic ulcer and halitosis.<sup>31–34</sup> In asthma patients however, breath ammonia concentration decreases.<sup>35</sup>

The average ammonia concentration in healthy individuals is approximately 250 ppb.

**Nitric oxide (NO).**—Nitric oxide (NO) has a critical role to play in the cell-signaling and its increased concentration in breath may be indicative of the pathophysiology of many diseases.<sup>36,37</sup> A large concentration of NO in exhaled breath is correlated with asthma. During asthma voluminous amounts of NO are produced in the airway by inducible-NOS (i-NOS). A healthy human being contains less than 25 ppb NO in breath, whereas in asthmatic patients it goes beyond 50 ppb.<sup>38</sup> Other than asthma, increased release of NO in human breath can be indicative of liver transplant rejection, chronic pulmonary obstructive disease and cystic fibrosis.<sup>39–42</sup>

**Hydrogen sulphide.**—Hydrogen sulphide is a well-known toxic gas with a malodor. It is a significant gasotransmitter in humans and animals signaling multiple physical processes such as, neuromodulation, cytoprotection, inflammation, apoptosis, vascular tone regulation etc.<sup>43–48</sup> Hydrogen sulphide may act as the biomarker of asthma,<sup>49</sup> airway inflammation,<sup>50,51</sup> and also oral and dental health.<sup>52</sup> The hydrogen sulphide concentration in healthy individuals ranges from 8–16 ppb.

**Acetone.**—Acetone was first recognized as the breath-biomarker of diabetes by Petters in 1857.<sup>53,54</sup> It should be understood clearly that glucose is the main source of energy in human body. Insulin allows glucose molecules to be absorbed in the cells. In case there is insufficient insulin generation by the body (Type-I diabetes) or insulin-resistance of the cells (Type-II diabetes) body is unable to extract energy from glucose and is compelled to break body fat to produce energy. Ketogenesis is one of such pathways. Ketogenesis is the source of all ketone bodies including acetone in humans. Figure 2 shows the basic steps involved in ketogenesis. Breath acetone concentration increases as the severity of diabetes in a patient escalates. The relation between blood and breath acetone is linear (acetone in exhaled air is approximately 1/330 times the acetone in plasma). For a non-diabetic person the breath acetone level is  $\leq 0.9$  ppm, for a moderately diabetic patient it is 0.9 ppm to 1.8 ppm and for seriously diabetic patients it can be several tens of

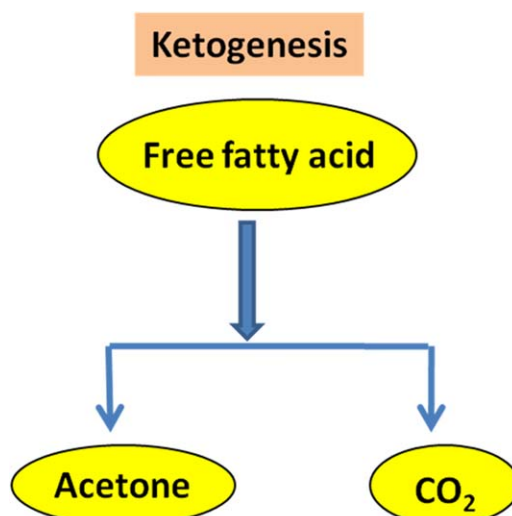


**Figure 2.** Production of acetone in human body by ketogenesis from free fatty acids.

ppm. Breath acetone level also increases in diabetic ketoacidosis, starvation, physical exercise and high fat/ketogenic diet.<sup>55,56</sup>

**Isoprene.**—Isoprene is present copiously in human breath. Isoprene, along with acetone acts as the biomarker of diabetes. Isoprene is a byproduct of cholesterol production in body and hence it can be potentially used as the biomarker for lipid metabolism disorder,<sup>8,57,58</sup> such as, anesthesia. When the concentrations of acetone, isoprene and methanol in breath are collectively lower than normal it might indicate lung cancer.<sup>14</sup> The concentration of isoprene in the breath of a healthy individual is approximately 105 ppb.

**Methane, ethane, pentane.**—Human bodies can not generate methane by themselves and Methanogenic bacteria (e.g. *Methanobrevibacter Smithii*) present in human intestine produces methane in anaerobic condition. Generally, methane is not present in human breath but in case of presence of excess methane generation it appears in the faeces and then it can also be detected in human breath also. The diseases caused by excess or less of methane in human body are obesity, irritable bowel syndrome, inflammatory bowel diseases, anorexia etc. Pentane and ethane are produced by the oxidation of cellular lipids.<sup>59</sup> Excess ethane in exhaled breath may be caused by oxidative stress, vitamin E deficiency, breast cancer, ulcerative colitis, whereas pentane in exhaled breath can be indicative of oxidative stress, physical and mental stress, arthritis, breast cancer, asthma, COPD, inflammatory bowel diseases, sleep apnea, ischemic heart disease, myocardial infarction, liver disease, schizophrenia, sepsis etc.<sup>60–69</sup>

**Aldehydes.**—Endogenous alkenals, hydroxyalkenals, and dialdehyde products of lipid peroxidation (LPO) tend to increase in cancer patients. LPO is a process where polyunsaturated fatty acids are peroxidised by free radicals and aldehydes could be reaction products. Patients with Wilson's disease, hemochromatosis associated with liver cancer, childhood cancer, alcoholic liver disease, smoking, oxidative stress, diabetes and atherosclerosis tend to have increased aldehyde levels in blood and breath.<sup>70</sup> Metabolic and/or genetic disorders in the synthesis and metabolism of aldehydes, such as, glyoxal, methylglyoxal, formaldehyde, semialdehydes etc. may lead to diabetes, hypertension, aging, Cerebral Ischemia,<sup>71,72</sup> Alzheimer's Disease (AD) and Parkinson's Disease (PD),<sup>73</sup> Amyotrophic Lateral Sclerosis (ALS) or Lou Gehrig's Disease,<sup>74</sup> Wernicke's Encephalopathy, lung cancer etc. When the concentration of such aldehydes increases in blood and urine its concentration in exhaled breath is also elevated. Thus, it can act as biomarker of multiple diseases, especially lung cancer.

Table I lists the major breath biomarkers along with the diseases they indicate.

### Techniques of Detecting Breath Biomarkers in Gas Phase

It is clear from the above discussions that human breath is a rich mixture of VOCs acting as biomarkers for different diseases and metabolic disorders. Therefore, detection of such VOCs in human breath can lead to potential non-invasive detection of diseases. In the following subsections we will discuss different methods developed to date to detect VOCs in very low concentrations (ppm<sub>v</sub>, ppb<sub>v</sub> and ppt<sub>v</sub>). Table I summarises the major diseases related to VOC biomarkers.

**Chromatographic and spectroscopic techniques.—Gas chromatography (GC).**—Chromatography is a method where a mixture of molecules of different compounds is forced by a carrier gas (generally He) through a column that separates the molecules<sup>75</sup> and the separated molecules are detected by a detector (ref. Fig. 3). In the last one decade or so, researchers across the globe are using GC combined with different kinds of detectors to detect breath VOCs for the purpose of disease detection and health monitoring. Sanchez et al.<sup>76</sup> detected about 25 components of human breath including important biomarkers such as, acetone, ethanol, isoprene, methanol, pentane using a series couple column ensemble [polar column stationary phase trifluoropropylmethylpolysiloxane or poly(ethylene glycol) and non-polar column stationary phase dimethyl polysiloxane] in combination with four-bed sorption trap and a flame ionization detector. The detection limit was 1–5 ppb in 0.8L of breath. Lord et al.<sup>77</sup> developed a GC-IMS based analytical system that could detect breath acetone and ethanol and obviated the effect of breath moisture to a large extent. Giardina et al.<sup>78</sup> developed a low temperature glassy carbon based solid-phase mass extraction micro-fiber that were capable of extracting five cancer related breath VOCs from simulated breath and the extracts were analyzed by GC/MS with good sensitivity. Phillips et al.<sup>79</sup> used GC-FID and GC-FPD (GC-flame photometric detection) techniques combined with a novel breath collection and preconcentration device to quantitatively detect isoprene from human breath with sufficient sensitivity, and accuracy. Lamote et al.<sup>80</sup> used GC-MS and e-Nose to differentiate between Malignant pleural mesothelioma (MPM) patients and asymptomatic asbestos-exposed person at a risk of the said disease. Schnabel et al.<sup>81</sup> employed GC-TOF-MS to show non-invasive detection of ventilator associated pneumonia (VAP) in ICU patients by breath VOC analysis and they identified 12 VOCs for that purpose. Beccaria et al.<sup>82</sup> employed thermal desorption-comprehensive two-dimensional gas chromatography-time of flight mass spectrometry methodology and chemometric techniques to detect pulmonary tuberculosis by analyzing exhaled breath VOCs. GC-MS was also employed by Durán-Acevedo et al.<sup>83</sup> to differentiate between healthy individuals and patients of gastric cancer by breath analysis using GC-MS. There are also other examples of such GC based breath analysis.

**Proton transfer reaction mass spectrometry (PTR-MS).**—PTR-MS is also a tool of analytical chemistry.<sup>84</sup> Classical PTR-MS uses gas phase hydronium ion as ion (purity >99.5%) source reagent. Using this technique absolute concentration of the target VOCs can be measured without calibration, the detection limits could be as low as ppt<sub>v</sub>. Figure 4 shows the block diagram of a PTR-MS. PTR-MS owing to its excellent sensitivity and specificity can be used for breath gas analysis to monitor the physiological and pathophysiological conditions of human subjects. Amann et al.<sup>85</sup> employed PTR-MS to investigate the variation in concentration of various VOCs during sleep (long-time, online monitoring combined with polysomnography), in patients with carbohydrate malabsorption (major role played by gut bacteria), and intra and inter-subject variability of one particular mass. Karl et al.<sup>86</sup> used PTR-MS to determine the level of isoprene in exhaled breath to detect cholesterologenesis

from exhaled breath. Lirk et al.<sup>87</sup> observed that potentially it is possible to screen head and neck squamous cell carcinoma using PTR-MS on exhaled breath VOCs using few biomarkers such as, isoprene. Boschetti et al.<sup>88</sup> reported to have simultaneously monitored a large number of VOCs in real time and with high sensitivity (tens to few ppt<sub>v</sub>).

**Selected mass flow tube mass spectrometry (SIFT-MS).**—SIFT-MS is a tool of analytical chemistry for the quantitative detection of trace VOCs.<sup>89</sup> Reagent ions, viz. H<sub>3</sub>O<sup>+</sup>, NO<sup>+</sup>, O<sub>2</sub><sup>+</sup> etc ionize the gas/VOC samples which are further quantified by a quadrupole mass spectrometer. Figure 5 shows the block diagram of a SIFT-MS. It was first developed to detect the trace VOCs present in human breath for prognosis of disease and to monitor physiological and pathophysiological conditions. Spanel et al.<sup>90</sup> used SIFT-MS and O<sub>2</sub><sup>+</sup> reagent ions to quantitatively detect isoprene in human breath. Diskin et al.<sup>91</sup> studied the variation in concentration of common breath biomarkers, such as ammonia, isoprene, ethanol, acetaldehyde and acetone over a period of 30 days using SIFT-MS with 5 healthy individuals. Abbott et al.<sup>92</sup> quantified acetonitrile from exhaled breath and urinary head space of many smokers and non-smokers. Vaira et al.<sup>93</sup> studied the relation between *Helicobacter pylori* concentration in the gut with gastrointestinal disease, liver disease, extra-gastrointestinal conditions, gastro-esophageal reflux etc. In 1996 itself, Smith et al.<sup>94</sup> used SIFT-MS to demonstrate that the breath ammonia concentration of a known *Helicobacter pylori* infected person increased by ~4 ppm after an oral dose of 2 g non-radioactive urea. Also, SIFT-MS was employed by Samara et al. (biomarker identified: acetone and pentane for acute decompensated heart failure), Cikach et al. (biomarker identified: isoprene and trimethylamine for acute decompensated heart failure), Alkhouri et al. (biomarker identified: acetone, isoprene, trimethylamine, acetaldehyde, pentane for non-alcoholic fatty liver disease), Hanounch et al. (biomarker identified: 2-propanol, ethanol, acetone, trimethylamine, acetaldehyde, pentane for alcoholic hepatitis), Walton et al. (biomarker identified: acetone for diabetes mellitus), Storer et al. (biomarker identified: acetone for diabetes mellitus)<sup>95–100</sup> and many others to explore non-invasive detection of diseases from exhaled breath.

**Nanomaterials for VOC detection.—Semiconductor oxides.**—In the previous section we have discussed about the spectroscopic techniques for breath analysis. In comparison to those techniques metal oxide semiconductor-based sensors provide multiple advantages, viz. small size, low cost, ease of operation, low power consumption, minimum maintenance requirements and overall simplicity. Thus, progressively increasing number of research groups around the globe are engaging themselves in the development of new metal oxide semiconductor (MOS) based sensor systems capable of detecting breath biomarkers of different diseases in breath background at concentration levels as low as ppm<sub>v</sub>, ppb<sub>v</sub> or even ppt<sub>v</sub>. To develop one such new composition it is important to understand the basic sensing mechanism of MOS sensors.

Gas sensing capability of MOS sensors completely depends on the change in electrical conductivity of the oxide material in response to the change in composition of the surrounding atmosphere. These sensors generally operate at high temperatures since oxide materials behave like insulators at room temperature, i.e. most of the electrons reside in the valence band and conduction band remains mostly empty. However, during synthesis defect bands are generated in the forbidden energy gap between the valence and conduction band. These defect bands could form either near the valence band as acceptor states or near the conduction band as donor states. The oxides having donor states are n-type MOS and those having acceptor states are p-type MOS. These defect states could have various origins, viz. defects in bulk oxide developed during synthesis process, high energy sites available in quantum dots, nanorods, nano sheets, nano tubes, nano belts and other exotic nanostructures, doping of novel and non-novel metals and oxides

**Table I. Biomarker vs Disease.**

| Biomarker                | Major disease   | Maximum permissible limit |
|--------------------------|---|---------------------------|
| Ammonia                  | Renal failure, liver dysfunction, cirrhosis of liver, peptic ulcer, halitosis etc   | 250 ppb                   |
| NO                       | Asthma, COPD, Asthma like diseases, viz. Laboratory animal allergy, lung infections in aluminium pot-room workers, swine confinement workers, lung cancer etc | 25 ppb                    |
| Hydrogen Sulphide        | Asthma, Airway inflammation, oral malodor, dental disease etc   | 8–16 ppb                  |
| Acetone                  | Diabetes  | 0.9 ppm                   |
| Isoprene                 | Diabetes, hypercholesterolemia  | 105 ppb                   |
| Methane, ethane, pentane | Intestine and colon related disease, breast cancer, liver diseases, asthma etc  | —                         |
| Aldehydes                | Cancers, viz. lung cancer, breast cancer, Alzheimer's disease, Parkinson's Disease, Wernicke's encephalopathy etc   | —                         |



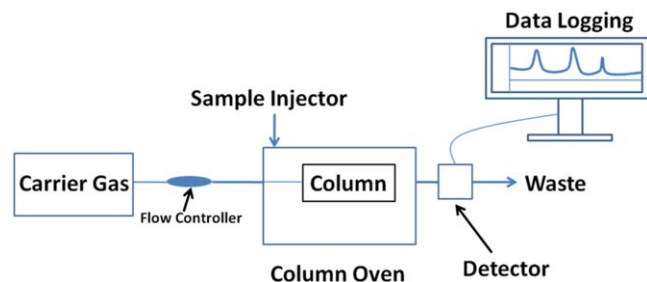


Figure 3. Block diagram of a Gas Chromatograph.

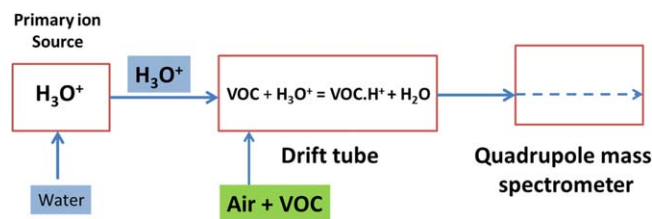
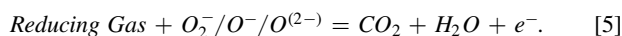
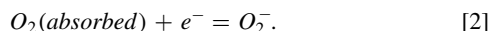
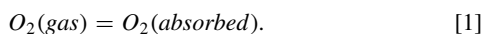


Figure 4. Block diagram of PTR-MS.

into the host lattice, band bending at the edges of particles in composite materials etc. At elevated temperatures (100 °C to 500 °C) electrons from the donor bands jump to the conduction band or from valence band to acceptor bands.<sup>101</sup> Ambient oxygen due to its electron affinity binds with these electrons and forms a variety of oxygen species with negative charges ( $O_2^-$ ,  $O^-$ , and  $O^{2-}$ ), thereby forming electron depletion layer (EDL) in n-type semiconductors and hole accumulation layer (HAL) in p-type semiconductors near the surface of the oxide.<sup>102</sup> When the surface is exposed to reducing gases such as  $NO_x$ ,  $NH_3$ , acetone, alcohol, isoprene etc ionosorbed oxygen at the surface oxidizes these molecules and thus gets consumed itself. Thus, the electrons previously trapped by these oxygen molecules are reverted back to the EDL or HAL and thus the conductivity increases or decreases, respectively. Thereafter, the ambient oxygen molecules recreate the EDL or HAL at the surface. Just the opposite happens when the material is exposed to oxidizing gases and VOCs. In essence, MOS behaves as n-type or p-type semiconductor at the elevated temperature. When the sensor is exposed to reducing gases, the resistance decreases for n-type oxides and increases of p-type oxides. The opposite phenomenon takes place in case the gas or VOC is oxidizing, viz.  $CO_2$ . Equations 1–5 describe the aforementioned phenomena for n-type MOS sensors. For p-type MOS sensors just the opposite phenomenon takes place.



From this brief discussion on the mechanism it is clear that the sensitivity of the sensors depends on the material composition, particle size, particle morphology, porosity of the sensor film, crystallographic planes exposed at the surface and film thickness. Doping and compositing the pristine material often increases sensitivity of the sensor. For example, surface modification of tin dioxide with palladium heightens the sensor response.<sup>103–109</sup> However, there is an optimum limit to that beyond which reduction in sensitivity is observed. Since the EDL and HAL forms at the surface itself, it is obvious that maximizing the surface area must increase the sensitivity. In thin films,<sup>110,111</sup> porous structures, 1-D<sup>112</sup> and 2-D<sup>113</sup> materials the exposed surface area is enhanced, therefore sensitivity increases significantly. Also, enhancing the reactivity at the surface will enhance sensitivity and that could be observed with 1-D, 2-D oxide particles and thin films.

Another important aspect of any sensor is selectivity. In general, the specificity of pristine oxide materials is not impressive. However, researchers have used various approaches to enhance selectivity, viz modulation of operating temperature,<sup>114</sup> noble-metal or oxide catalyst loading,<sup>115,116</sup> acid-base interaction between target gases/VOCs and the MOS,<sup>117</sup> reforming the target gases within the sensing layer,<sup>118,119</sup> interface-gas filtration<sup>120</sup> etc. The effect of some major parameters on sensitivity and selectivity are discussed in details in the latter part of this section.

Power consumption is a limitation of thick film MOS sensors. One of the major advantages of such sensors is that it could be used for making hand-held devices. A hand-held device is essentially battery operated. However, a standard thick film MOS sensor consumes about 0.5 W to 1 W power. Such power consumption is difficult to be sustained for prolonged times using batteries. Also, the current drawn by the circuit is of the order of 100–300mA which is quite high and requires sophisticated electronic circuitry to handle it. Also, during prolonged use it heats up the air in the vicinity and creates turbulence there. This hinders the streamlined flow of analyte gases onto the surface of the sensor, especially when breath gas analysis is concerned. It is difficult to get repeatable results under such conditions. Lowering the operating temperature could be one solution but it comes with other allied problems such as, low selectivity, slow response and recovery, unstable base resistance etc. This necessitates the introduction of MEMS based thin film sensors which have higher sensitivity, lower resistance, lower power consumption and eventually consumes much less physical space. The advent of MEMS and NEMS based sensors also opens up the horizon to hand held sensor array-based devices. Sensor arrays are one of the best solutions to the selectivity issue of such sensors.

Following are some of the recently developed MOS sensors having the potential of being used in breath biomarker detection.

Tungsten oxide ( $WO_3$ ) has been identified as a potential MOS for the detection of NO in ppm and ppb levels. Moon et al.<sup>121</sup> reported

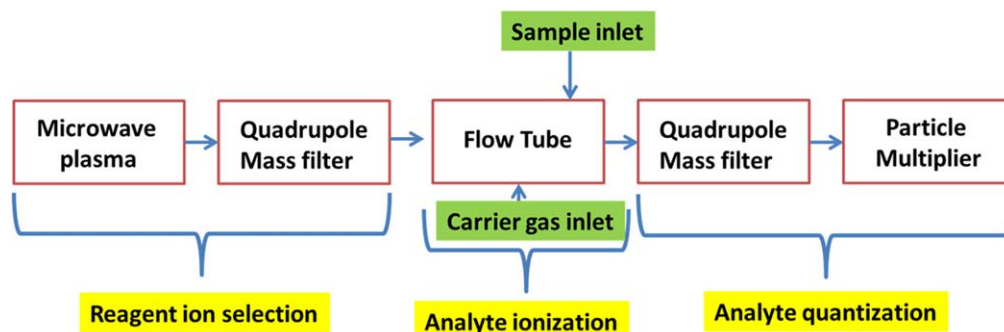


Figure 5. Block diagram of SIFT-MS.

that villi-like  $\text{WO}_3$  is capable of detecting down to 200 ppb NO. Koo et al.<sup>122</sup> reported that nanotubes of  $\text{WO}_3$  are capable of detecting 1 ppb NO in high humidity (>80%). Sun et al.<sup>123</sup> used sensor design with the adjacent alignment of p-type chromium oxide ( $\text{Cr}_2\text{O}_3$ ) and n-type  $\text{WO}_3$  to detect down to 18 ppb NO in presence of 20 ppm CO. Their study was even extended to detection of NO in human breath samples. Zhang et al.<sup>124</sup> observed the selective sensing of  $\text{NO}_2$  by ZnO hollow spheres-based sensors. Gouma et al.<sup>125</sup> reported that  $\gamma\text{-WO}_3$  is a selective NO sensor in presence of other breath volatiles, viz. acetone, isoprene, ethanol, CO and methanol. Fruhberger et al.<sup>126</sup> reported that  $\text{WO}_3$  based sensor can detect down to 60 ppm NO when passed through an oxidizing filter of alumina supported potassium permanganate. However, it seems that far more studies have to be carried out in this regard. The detection of  $\text{NO}_x$  becomes difficult considering that  $\text{NO}_x$  is a common air pollutant. Also,  $\text{NO}_x$  concentration is very high in children (~450 ppb as compared to ~30 ppb in non-asthmatic adults). Therefore, it is difficult to detect asthma by detection of  $\text{NO}_x$  in exhaled breath in children. Furthermore, adults having stabilized asthma exhibits ~20–25 ppb  $\text{NO}_x$  in exhaled breath which is not so different from non-asthmatic individuals.  $\text{NO}_x$  measurement in humid conditions has also not been done exhaustively. These lacunas should be filled in by the future researchers. Table II summarises the major research contributions in trace NO detection.

Ammonia concentration in the exhaled breath of healthy human beings range from 425–1800 ppb with a mean of 960 ppb. Molybdenum oxide and tungsten oxide have exhibited high selectivity towards ammonia. Mutschall et al.<sup>127</sup> reported that reactively sputtered thin film of rhombic  $\text{MoO}_3$  can detect ammonia at temperatures of 400 °C–450 °C. Imawan et al.<sup>128</sup> reported that use of Ti overlayers on sputtered  $\text{MoO}_3$  thin films can enhance the sensitivity and selectivity towards ammonia while reducing cross-sensitivity towards carbon monoxide, sulphur dioxide and hydrogen. Sunu et al.<sup>129</sup> suggested that ammonia sensing mechanism of  $\text{MoO}_3$  involves formation of molybdenum suboxide and nitrides. Gouma et al.<sup>130</sup> was able to detect down to 50 ppb ammonia employing spin coated  $\text{MoO}_3$  synthesized by sol-gel route. Jodhani et al.<sup>131</sup> could measure down to 500 ppb ammonia using flame spray synthesized pristine  $\alpha\text{-MoO}_3$  Nanosheets. Prasad et al.<sup>132</sup> compared ammonia sensing properties of sol-gel prepared and ion beam deposited  $\text{MoO}_3$  thin films. It was revealed that ion beam deposited thin films could detect ammonia down to 3 ppm, whereas the sol-gel deposited thin films could detect down to 8 ppm ammonia. Very recently, Kwak et al.<sup>133</sup> reported to have detected ammonia down to 280 ppt using hydrothermally synthesized  $\alpha\text{-MoO}_3$  nanoribbons ( $\text{MoO}_3$  NRs). However, most of these tests were conducted at dry atmospheres, whereas exhaled human breath contains almost saturated moisture. Also, the ammonia sensing properties of  $\text{MoO}_3$  is given to acid-base interaction, which might be adversely affected at high %RH conditions, thereby affecting the sensitivity and selectivity of the sensor. Gunter et al.<sup>134</sup> fabricated a chemoresistive gas sensor based on Si-stabilized  $\alpha\text{-MoO}_3$  made by flames and it could sense ammonia down to 400 ppb even at 90% relative humidity. This research is therefore very important and more of future research needs to focus on this problem.

Srivastava et al.<sup>135</sup> reported that  $\text{WO}_3$  thick film with a over-coating of Pt catalyzed silica-niobia layer could detect down to 15 ppm ammonia at 450 °C with a response time of less than 30 s.

**Table II. Detection of NO using semiconductor metal oxides.**

| Nanomaterial                        | Morphology    | Lowest concentration of NO detected |
|-------------------------------------|---------------|-------------------------------------|
| $\text{WO}_3$                       | Villi-like    | 200 ppb <sup>121</sup>              |
| $\text{WO}_3$                       | Nanotube      | 1 ppb <sup>122</sup>                |
| $\text{WO}_3/\text{Cr}_2\text{O}_3$ | NA            | 18 ppb <sup>123</sup>               |
| ZnO                                 | Hollow sphere | 10 ppm $\text{NO}_2$ <sup>124</sup> |
| $\gamma\text{-WO}_3$                | NA            | 10 ppm <sup>125</sup>               |
| $\text{WO}_3$                       | Thin film     | 60 ppm <sup>126</sup>               |

Jimenez et al.<sup>136</sup> reported that 5%Cr doped  $\text{WO}_3$  shows excellent response to 500 ppb ammonia. Earlier, Jimenez et al.<sup>137</sup> reported the ammonia sensing properties of Cu (0.2% and 2%) and V (0.2% and 2%) doped  $\text{WO}_3$ . Comparing these two reports it seems that Cr doping increases the sensitivity to ammonia more than Cu or V. Zamani et al.<sup>138</sup> reported that chemically prepared mesoporous 2% Cr doped  $\text{WO}_3$  deposited on a MEMS platform was capable of detecting 5 ppm ammonia with highest sensitivity observed at 350 °C. Jeevitha et al.<sup>139</sup> prepared porous rGO/ $\text{WO}_3$  nanocomposite that could detect ammonia down to 1.14 ppm at room temperature (32 °C–35 °C) and 55% relative humidity. Wu et al.<sup>140</sup> detected ammonia down to 5 ppm with tin monoxide nanoshells with a p-type response of 313%. Zhang et al.<sup>141</sup> prepared ZnO/ $\text{MoS}_2$  nanocomposite which comprised of ZnO nanorods and  $\text{MoS}_2$  nanosheets. The sensor could detect down to 500 ppb ammonia. Table III summarises the major research contributions in trace ammonia detection.

As already discussed, acetone is considered to be the breath biomarker of diabetes. Amongst all the nano-materials capable of detecting acetone in the form of VOC, semiconductor oxides top the list. The two major oxides showing maximum response to acetone are  $\text{WO}_3$  (tungsten oxide) and  $\text{Fe}_2\text{O}_3$  (iron oxide). Choi et al.<sup>160</sup> reported that Pt functionalized  $\text{WO}_3$  hemitube with wall thickness of 60 nm exhibited superior sensitivity to acetone ( $R_{\text{air}}/R_{\text{gas}} = 4.11$  at 2 ppm) with a detection limit of 120 ppb and 7 month stability. In another paper Choi et al.<sup>161</sup> demonstrated that Pt loaded porous  $\text{WO}_3$  nanofiber showed excellent sensitivity to acetone with response of 28.9 [ $R_{\text{air}}/R_{\text{gas}}$ ] to 5 ppm acetone vapor. Kim et al.<sup>162</sup> reported the excellent acetone sensitivity ( $R_{\text{air}}/R_{\text{gas}} = 62$  at 1 ppm) of apoferritin encapsulated Pt doped electro-spun meso-porous  $\text{WO}_3$ . Righettoni et al.<sup>163</sup> reported an ultrasensitive Si doped  $\varepsilon\text{-WO}_3$  sensor which had a detection limit of 20 ppb and could differentiate between 0.9 ppm and 1.8 ppm acetone vapor even at 90%RH at 400 °C operating temperature. In another literature, Righettoni et al.<sup>164</sup> demonstrated that 10 mol% silica ( $\text{SiO}_2$ ) doped  $\text{WO}_3$  can have a detection lower limit of 20 ppb to acetone. In yet another literature Righettoni et al.<sup>165</sup> compared the results of Si doped  $\text{WO}_3$  and PTR-MS in detecting acetone in real human breath and appreciable correlation was demonstrated. Recently, Kim et al.<sup>164</sup> reported that apoferritin modified ruthenium oxide quantum dots ( $\text{Ru}_2\text{O}$ ) functionalized, electrospun  $\text{WO}_3$  nanofibers can effectively detect acetone vapor ( $R_{\text{air}}/R_{\text{gas}} = 78.61$  at 5 ppm) even at 95% RH. Earlier the same group<sup>165</sup> reported that  $\text{Rh}_2\text{O}_3$ -decorated  $\text{WO}_3$  nanofibers has a sensing response of  $R_{\text{air}}/R_{\text{gas}} = 41.2$  at 5 ppm acetone vapor at highly humid conditions (95% RH). Xu et al.<sup>166</sup> reported that electrospun  $\text{WO}_3$  based hierarchical structure with mesopores of uniform and controlled sizes and interconnected channels prepared by sacrificial templates of silica and polyvinylpyrrolidone (PVP) can detect sub-ppm (<1 ppm) acetone.

Another very important oxide in trace acetone detection is iron oxide. Sen et al.<sup>167</sup> patented a Pt and antimony oxide ( $\text{Sb}_2\text{O}_3$ ) doped  $\gamma\text{-iron oxide}$  ( $\gamma\text{-Fe}_2\text{O}_3$ ) composition that could effectively detect down to 1 ppm acetone even in humid conditions. Cheng et al.<sup>168</sup> reported the trace acetone sensing behavior of Eu-doped  $\alpha\text{-iron oxide}$  nanotubes and nanowires. It was observed through their study that the Eu doped  $\alpha\text{-Fe}_2\text{O}_3$  nanotube has a superior sensitivity (about 2.7 times) over the nanowires at 100 ppm of acetone. The detection limit was 0.1 ppm with fast response and recovery.

There are other miscellaneous oxides which have shown excellent sensitivity to ppm(v) to ppb(v) acetone vapor. For example, Narjinary et al.<sup>169</sup> showed that a sol-gel derived composite of tin-di-oxide ( $\text{SnO}_2$ ) and multiwalled CNT could efficiently detect acetone down to 1 ppm with sufficiently fast response and recovery time. Chakraborty et al.<sup>170</sup> reported that sol-gel derived bismuth ferrite nanoparticles could detect down to 1 ppm acetone with an appreciable sensitivity of  $R_{\text{air}}/R_{\text{gas}} = 1.8$  at 350 °C. She also explained the plausible underlying mechanism. Abokifa et al.<sup>171</sup> were able to detect acetone at room temperature using tin dioxide nanocolumns prepared by aerosol-route. The experimental results were validated using density functional theory based theoretical modeling. Priya et al.<sup>172</sup> observed that 2 wt%

**Table III. Detection of NH<sub>3</sub> using semiconductor metal oxides.**

| Nanomaterial  | Morphology  | Lowest concentration of NH <sub>3</sub> detected |
|---|---|--|
| Rhombic MoO <sub>3</sub>  | Reactively sputtered thin film                        | 25 ppm <sup>127</sup>                            |
| MoO <sub>3</sub> with Ti overlayer  | Sputtered thin film                                   | 50 ppm <sup>128</sup>                            |
| Spin coated MoO <sub>3</sub>  | NA  | 50 ppb <sup>130</sup>                            |
| α-MoO <sub>3</sub>  | Nanosheets  | 500 ppb <sup>131</sup>                           |
| α-MoO <sub>3</sub>  | Ion beam deposited                                    | 3 ppm <sup>132</sup>                             |
| α-MoO <sub>3</sub>  | Nanoribbons   | 280 ppt <sup>133</sup>                           |
| Si doped α-MoO <sub>3</sub>   | Needle like morphology                                | 400 ppb <sup>134</sup>                           |
| WO <sub>3</sub> thick film with a overcoating of Pt catalyzed silica-niobia layer | NA  | 15 ppm <sup>135</sup>                            |
| 5wt% Cr doped WO <sub>3</sub>   | NA  | 500 ppm <sup>136</sup>                           |
| V and Cu doped WO <sub>3</sub>  | NA  | 500 ppm <sup>137</sup>                           |
| 2wt% Cr doped WO <sub>3</sub>   | Mesoporous nanoparticle                               | 5 ppm <sup>138</sup>                             |
| Pt and Cr-doped WO <sub>3</sub> thin films  | Mesoporous nanoparticle                               | 6.2 ppm <sup>142</sup>                           |
| rGO/ WO <sub>3</sub> nanocomposite  | Porous nanosheets with nano-spherical WO <sub>3</sub> | 1.14 ppm <sup>139</sup>                          |
| SnO <sub>2</sub>  | nano-shell  | 5 ppm <sup>140</sup>                             |
| ZnO/MoS <sub>2</sub>  | Self-assembled  | 500 ppb <sup>141</sup>                           |
| Pure and Pt-doped WO <sub>3</sub>   | Nanoparticle  | 100 ppm <sup>143</sup>                           |
| Pure and Pt loaded WO <sub>3</sub>  | Mesoporous  | 50 ppm <sup>144</sup>                            |
| WO <sub>3</sub>   | Nanowire  | 1500 ppm <sup>145</sup>                          |
| Pure & Cr and Pt doped WO <sub>3</sub>  | Macroporous   | 6.2 ppm <sup>146</sup>                           |
| WO <sub>3</sub>   | Nanorods  | 50 ppm <sup>147</sup>                            |
| W <sub>18</sub> O <sub>49</sub>   | Nanowire  | 100 ppb <sup>148</sup>                           |
| Polypyrrole -WO <sub>3</sub> composite  | Nanofiber   | 1 ppm <sup>149</sup>                             |
| WO <sub>3</sub>   | Nanofiber   | 50 ppm <sup>150</sup>                            |
| Pure and Cr-WO <sub>3</sub>   | NA  | 50 ppm <sup>151</sup>                            |
| WO <sub>3</sub>   | Nanorods  | 25 ppm <sup>152</sup>                            |
| rGO-SnO <sub>2</sub> composite films  | NA  | 25 ppm <sup>153</sup>                            |
| bilayer thin film of SnO <sub>2</sub> -WO <sub>3</sub>                            | NA  | 50 ppm <sup>154</sup>                            |
| PANI/WO <sub>3</sub> composite  | NA  | 10 ppm <sup>155</sup>                            |
| SnO-PANI nanocomposite  | NA  | 100 ppm <sup>156</sup>                           |
| rGO/WS <sub>2</sub> heterojunction  | NA  | 10 ppm <sup>157</sup>                            |
| Flexible graphene based wearable gas sensor                                       | NA  | ppt level <sup>158</sup>                         |
| ZnO with functionalized CNT and Graphite  | NA  | ~40 ppm <sup>159</sup>                           |



Au doped electrospun SnO<sub>2</sub> exhibited trace acetone sensing at 250 °C. Also, spray deposited gallium doped SnO<sub>2</sub> has been reported to detect low ppm acetone vapor at 350 °C.<sup>173</sup> 2 wt% Ni doped zinc oxide thin film acetone sensor prepared by spray pyrolysis method was reported by Khalidi et al.<sup>174</sup> Hydrothermally prepared Pt-functionalized nanoporous titania (TiO<sub>2</sub>) was reported to detect acetone in ppm(v) level by Xing et al.<sup>175</sup> Electrospun indium oxide (In<sub>2</sub>O<sub>3</sub>) nanowire with a controllable Pt core was prepared by Liu et al.<sup>176</sup> and it could detect down to 10 ppb acetone vapor. It had a fast dynamic process, good selectivity and long-term stability. The molecular sieve employed decreases the deleterious effect of moisture to a great extent. The authors claimed that this sensor has the potential of becoming an inexpensive, simple, non-invasive diabetes detector. To develop humidity-independent acetone sensor Yoon et al.<sup>177</sup> decorated hollow In<sub>2</sub>O<sub>3</sub> spheres with CeO<sub>2</sub> nanoclusters. It was demonstrated that indium oxide spheres with ≥11.7 wt% cerium oxide surface loading results into excellent humidity-independent acetone sensing. Jang et al.<sup>178</sup> developed apoferritin modified Pt-functionalized, highly porous SnO<sub>2</sub> by electrospinning method using polyvinylpyrrolidone (PVP) and polystyrene (PS) as sacrificial pore formers. The functional material so developed has excellent sensitivity ( $R_{\text{air}}/R_{\text{gas}} = 192$  at 5 ppm) and lowest detection limit of 10 ppb. Shin et al.<sup>179</sup> developed thin walled, assembled SnO<sub>2</sub> nanofibers with wrinkled layers and elongated channel like pores and voids that enhanced the sensitivity towards acetone with respect to densely packed SnO<sub>2</sub> nanofibers. Also, surface decoration with Pt nanoparticles markedly enhances the sensitivity. The lowest detection limit was reported to be 120 ppb of acetone vapor. Also, Koo et al.<sup>180</sup> reported that Pd doped ZnO/ZnCo<sub>2</sub>O<sub>4</sub> hollow spheres prepared by metal-organic template method has notable sensitivity and selectivity to trace acetone (69% sensitivity to 5 ppm acetone at 250 °C).

Humidity and ethanol in breath are two major cross-sensitive agents that might hinder the efficacy of a metal oxide acetone vapor sensor from exhaled breath. In many of the abovementioned works the effect of humidity has been nullified or reduced to a great extent by increasing the operating temperature, using a moisture trap, or just by tuning the composition and morphology. However, further developments in this regard are necessary. Ethanol concentration in the breath of a healthy individual is generally much lower than that of acetone. However, for an intoxicated person it ramps up to 100 s of ppm. That can hinder the selective detection of acetone. In this regard acidic oxides, such as tungsten oxide (WO<sub>3</sub>) have proven better than the basic oxides. However, more work needs to be done in this field. Table IV summarises the major research contributions in trace acetone detection.

As already mentioned in Table I; hydrogen sulphide (H<sub>2</sub>S) is a breath biomarker for halitosis. The major oxides that can detect trace H<sub>2</sub>S (<1 ppm range) are copper oxide (CuO), tin dioxide (SnO<sub>2</sub>), indium oxide (In<sub>2</sub>O<sub>3</sub>), zinc oxide (ZnO), titanium oxide (TiO<sub>2</sub>) and iron oxide (Fe<sub>2</sub>O<sub>3</sub>). Steinhauer et al.<sup>201</sup> developed CuO nanowires by on chip thermal oxidation of electroplated Cu and these nanowires owing to their high surface to volume ratio could detect down to 10 ppb H<sub>2</sub>S. Vertically aligned CuO nanowire array based sensor prepared by in situ SEM micro-manipulation was employed by Chen et al.<sup>202</sup> to detect down to 500 ppb H<sub>2</sub>S. CuO nanosheets were developed by Zhang et al.<sup>203</sup> for selective and sensitive detection of trace H<sub>2</sub>S down to 2 ppb. It is worth mentioning that this material exhibited strong recovery. Ramgir et al.<sup>204</sup> prepared CuO thin films by oxidation of Cu film deposited by thermal evaporation technique and this material was capable of detecting sub-ppm H<sub>2</sub>S. Importantly, at low concentrations of 100–400 ppb the response and recovery were reasonably fast, 60 s and 90 s, respectively. Hierarchical hollow porous sphere of CuO were developed by Qin et al.<sup>205</sup> The sensor showed excellent detection lower limit (2 ppb), response (3 s) and recovery (9 s) time towards H<sub>2</sub>S.

About two decades ago, Tamaki et al.<sup>206</sup> reported that a thin film sensor prepared from a composite of CuO-SnO<sub>2</sub> could detect 0.02 ppm H<sub>2</sub>S at 300 °C. Similarly, CuO loaded SnO<sub>2</sub> nanowires

were developed by Giebelhaus et al.<sup>207</sup> for enhancing the sensitivity towards H<sub>2</sub>S. The p-n heterojunction formed at the CuO-SnO<sub>2</sub> interface was responsible for the enhanced detection ability of the material. Xue et al.,<sup>208</sup> also hypothesized that the p-n junction developed at the interface of CuO-SnO<sub>2</sub> core/shell structure developed by them, was responsible for the heightened H<sub>2</sub>S sensing ability of the sensing material. Similar composite was also developed by Hwang et al.<sup>209</sup> In their work they reported that CuO sensitized SnO<sub>2</sub> nanowire showed 74 times higher sensitivity than SnO<sub>2</sub> nanowire alone at 20 ppm H<sub>2</sub>S. The recovery time was short (1–2 s) and the cross-sensitivity to NO<sub>2</sub>, CO, ethanol and C<sub>3</sub>H<sub>8</sub> were also negligible. Choi et al.<sup>210</sup> had similar findings with CuO decorated SnO<sub>2</sub> hollow spheres. Sb-doped SnO<sub>2</sub> capable of detecting 100 ppb H<sub>2</sub>S at room temperature was reported by Ma et al.<sup>211</sup>

CuO decoration is found to be effective for selective H<sub>2</sub>S detection also on In<sub>2</sub>O<sub>3</sub>. Liang et al.<sup>212</sup> reported that CuO loaded In<sub>2</sub>O<sub>3</sub> nanowires can effectively detect low concentrations, viz. 5 ppm of hydrogen sulphide selectively with respect to NO<sub>2</sub>, H<sub>2</sub>, CO, NH<sub>3</sub>, C<sub>2</sub>H<sub>5</sub>OH, C<sub>3</sub>H<sub>8</sub>O, TMA, C<sub>7</sub>H<sub>8</sub>, and C<sub>8</sub>H<sub>10</sub> at room temperature and 150 °C. The high surface area of the 1-D nano-structure and the abundance of p-n heterojunction formed at the interface of the two oxides have been pointed out as the reasons for such high sensitivity and selectivity.

Hollow spheres of ZnO-CuO prepared by hydrothermal method also revealed high response to 5 ppm H<sub>2</sub>S and negligible cross-response to much higher concentrations of C<sub>2</sub>H<sub>5</sub>OH, C<sub>3</sub>H<sub>8</sub>, CO and H<sub>2</sub> at 336 °C.<sup>213</sup> In this paper also, Kim et al. pointed out the abundance of p-n heterojunctions formed at the ZnO-CuO interface within the hollow spheres as the plausible sensing mechanism. Wo et al.,<sup>214</sup> reported that Mo-doped ZnO nanowire network sensors displayed excellent sensitivity to 5 ppm H<sub>2</sub>S ( $R_{\text{a}}/R_{\text{g}} = 14.11$ ) with negligible cross-sensitivity to C<sub>2</sub>H<sub>5</sub>OH, NH<sub>3</sub>, HCHO, CO, H<sub>2</sub>, *o*-xylene, benzene, toluene, and trimethylamine at the same concentration level. Mo decoration at the surface effectively increases the sensitivity and selectivity to H<sub>2</sub>S. A novel cage-like ZnO-MoO<sub>3</sub> composite was developed by hydrothermal method by Yu et al.<sup>215</sup> for detection of trace H<sub>2</sub>S down to 500 ppb. MoO<sub>3</sub> itself turns up as a selective and sensitive H<sub>2</sub>S sensor. Excellent response to H<sub>2</sub>S in air down to 5 ppm was observed by Galstyan et al.<sup>216</sup> using long chains (≤30 μm) of ZnO nanobeads prepared by anodic oxidation of sputtered Zn film followed by oxidation. Hydrothermally synthesized ZnO nanorods capable of detecting down to 0.05 ppb H<sub>2</sub>S was reported by Wang et al.<sup>217</sup>

Free-standing, semi-transparent, flexible MoO<sub>3</sub> nanopaper was utilized by Li et al. to detect H<sub>2</sub>S down to 0.25 ppm.<sup>218</sup> A MoO<sub>3</sub>-Fe<sub>2</sub>(MoO<sub>4</sub>)<sub>3</sub> core-shell composite that could detect down to 1 ppm H<sub>2</sub>S was developed by Gao et al.<sup>219</sup> Mo doped SnO<sub>2</sub> thick-film developed by Kabcum et al.<sup>220</sup> was capable of detecting down to 0.25 ppm H<sub>2</sub>S. SnO<sub>2</sub> yolk-shell nanostructure with uniform Ag surface-loading prepared by Yoon et al.<sup>221</sup> also exhibited excellent sensitivity towards H<sub>2</sub>S ( $R_{\text{a}}/R_{\text{g}} - 1 = 613.9$ , to 5 ppm H<sub>2</sub>S). Ag doping worked well with TiO<sub>2</sub> also. Ma et al.<sup>222</sup> discovered that the said nanostructure could detect down to 1 ppm H<sub>2</sub>S.

Further, low-temperature Ag-doped α-Fe<sub>2</sub>O<sub>3</sub> based H<sub>2</sub>S sensor capable of detecting down to 50 ppm H<sub>2</sub>S was developed by Wang et al.<sup>223</sup> Tian et al.<sup>224</sup> reported that hierarchical, hollow nano-boxes of Fe<sub>2</sub>O<sub>3</sub> were capable of detecting down to 0.25 ppm H<sub>2</sub>S with sufficiently fast response and recovery time. Ultrasensitive low-ppm H<sub>2</sub>S sensor was prepared by Ma et al.<sup>225</sup> using nano-chains of α-Fe<sub>2</sub>O<sub>3</sub>. Balouria et al.<sup>226</sup> could detect ~10 ppm H<sub>2</sub>S using Au modified Fe<sub>2</sub>O<sub>3</sub> thin films.

WO<sub>3</sub> is another potential candidate for detection of traces of H<sub>2</sub>S from gas phase. Lonescu et al.<sup>227</sup> prepared a semi-thin film (~20 μm) of WO<sub>3</sub> quantum dots (5nm diameter) that could detect down to 20 ppb H<sub>2</sub>S. Pd functionalized highly porous WO<sub>3</sub> nanofiber was reported to be a potential candidate for the detection of halitosis and lung cancer from breath.<sup>228</sup> Gold incorporated vacuum deposited WO<sub>3</sub> thin film was observed to be detecting 100 ppb H<sub>2</sub>S.<sup>229</sup>

**Table IV. Detection of acetone using semiconductor metal oxides.**

| Nanomaterial   | Morphology  | Lowest concentration of acetone detected |
|--|---|--|
| Pt functionalized WO <sub>3</sub>  | Hemitube  | 120 ppb <sup>160</sup>                   |
| Pt functionalized WO <sub>3</sub>  | Porous nanofiber  | 5 ppm <sup>161</sup>                     |
| Pt doped WO <sub>3</sub>   | Mesoporous  | 1 ppm <sup>162</sup>                     |
| Si doped $\epsilon$ -WO <sub>3</sub>   | NA  | 20 ppb at 90%RH <sup>109</sup>           |
| Ru <sub>2</sub> O functionalized WO <sub>3</sub>                                     | Nanofiber   | 5 ppm at 95%RH <sup>164</sup>            |
| Rh <sub>2</sub> O <sub>3</sub> -decorated WO <sub>3</sub>                            | Nanofiber   | 5 ppm at 95%RH <sup>165</sup>            |
| WO <sub>3</sub>  | Mesoporous  | <1 ppm <sup>166</sup>                    |
| Pt and Sb <sub>2</sub> O <sub>3</sub> doped $\gamma$ -Fe <sub>2</sub> O <sub>3</sub> | Spherical nanoparticles   | 1 ppm <sup>167</sup>                     |
| Eu doped $\alpha$ -Fe <sub>2</sub> O <sub>3</sub>                                    | Nanotubes   | 100 ppb <sup>168</sup>                   |
| SnO <sub>2</sub> -MWCNT nanocomposite  | Spherical nanoparticles and tubular CNTs  | 1 ppm <sup>169</sup>                     |
| Bismuth Ferrite  | Spherical nanoparticles   | 1 ppm <sup>170</sup>                     |
| Au doped SnO <sub>2</sub>  | Nanofiber   | 2 ppm <sup>172</sup>                     |
| Y doped SnO <sub>2</sub>   | Prismatic hollow nanofiber  | 20 ppm <sup>181</sup>                    |
| Ga doped SnO <sub>2</sub>  | Thin film   | 6000 ppm <sup>173</sup>                  |
| Eu doped SnO <sub>2</sub>  | Nanobelt  | 100 ppm <sup>182</sup>                   |
| Ni doped SnO <sub>2</sub>  | NA  | 200 ppm <sup>183</sup>                   |
| Co doped SnO <sub>2</sub>  | Thin film   | 0.1 ppm <sup>184</sup>                   |
| Ni and Ce doped SnO <sub>2</sub>   | Thin film   | 100 ppm <sup>185</sup>                   |
| rGO doped SnO <sub>2</sub>   | Nanofiber   | 5 ppm <sup>186</sup>                     |
| SnO <sub>2</sub> /Au-doped In <sub>2</sub> O <sub>3</sub> heterojunction             | Coaxial nanofiber   | 5 ppm <sup>187</sup>                     |
| $\alpha$ -Fe <sub>2</sub> O <sub>3</sub> /SnO <sub>2</sub>                           | NA  | 100 ppm <sup>188</sup>                   |
| SnO <sub>2</sub> -ZnO  | Hetero-nanofiber  | 100 ppm <sup>189</sup>                   |
| SnO <sub>2</sub> -TiO <sub>2</sub>   | NA  | 200 ppm <sup>190</sup>                   |
| SnO <sub>2</sub>   | Nanowires   | 20 ppm <sup>191</sup>                    |
| SnO <sub>2</sub>   | Hollow microsphere  | 50 ppm <sup>192</sup>                    |
| SnO <sub>2</sub>   | Nanotube  | 20 ppm <sup>193</sup>                    |
| SnO <sub>2</sub>   | Aurelia   | 10 ppm <sup>194</sup>                    |
| SnO <sub>2</sub>   | Thin film   | 8 ppm <sup>195</sup>                     |
| SnO <sub>2</sub>   | Nanobelt  | 5 ppm <sup>196</sup>                     |
| Au:SmFe <sub>0.9</sub> Zn <sub>0.1</sub> O <sub>3</sub>                              | Nanoparticle  | 0.01 ppm <sup>197</sup>                  |
| Ca <sup>2+</sup> and Au co-doped SnO <sub>2</sub>                                    | Nanofiber   | 10 ppm <sup>198</sup>                    |
| Pt functionalized SnO <sub>2</sub>   | Porous nanotubes  | 10 ppb <sup>178</sup>                    |
| Pt functionalized SnO <sub>2</sub>   | Thin wall, assembled nanofiber  | 120 ppb <sup>179</sup>                   |
| Ni doped ZnO   | Thin film   | 100 ppm <sup>174</sup>                   |
| Pt doped ZnO   | Nanoparticle  | 50 ppm <sup>199</sup>                    |
| Nb doped ZnO   | Nanoparticle  | 50 ppm <sup>199</sup>                    |
| V doped ZnO  | Thin film   | 100 ppm <sup>200</sup>                   |
| Pt-functionalized TiO <sub>2</sub>   | Nanoporous  | 200 ppm <sup>175</sup>                   |
| In <sub>2</sub> O <sub>3</sub> with controllable Pt core                             | Nanowire  | 10 ppb <sup>176</sup>                    |
| CeO <sub>2</sub> decorated In <sub>2</sub> O <sub>3</sub>                            | Hollow spheres of In <sub>2</sub> O <sub>3</sub> , CeO <sub>2</sub> nanocluster | 500 ppb <sup>177</sup>                   |

There are multiple other oxides, composites and doped/decorated oxides viz. Co<sub>3</sub>O<sub>4</sub>,<sup>230</sup> BaTiO<sub>3</sub>,<sup>231</sup> YMnO<sub>3</sub>,<sup>232</sup> CdIn<sub>2</sub>O<sub>4</sub>,<sup>233</sup> lanthanum lead iron nickel oxide, iron doped calcium copper titanate<sup>234</sup> etc that are capable of detecting H<sub>2</sub>S gas in ppb to 1000 ppm level.

From the above discussion it is clear that the pristine and composited CuO based sensors have the highest potential for detecting hilatosis from breath. Through the discussion of the literatures it is evident that the sensitivity and selectivity can be increased by increasing the surface to volume ratio, increasing the porosity so the target analyte can reach most of the active sites of the functional material and by increasing the number of p-n junctions. So this could be the model for the researchers working in this area. Also, Mo due to its tendency to easily form MoS<sub>2</sub> has been another potential candidate. The major concern in this regard is slow recovery time of most of the sensors that need to improve through future research activities. Also, the quest for novel materials that may stand up to the purpose are in vogue. Table V summarises the major research contributions in trace H<sub>2</sub>S detection.

Available literature suggests that amongst all the cancers, lung cancer has the highest possibility of being detected by VOC analysis by semiconductor metal oxides. By far ~30 VOCs have been detected that can collectively be considered as the breath biomarkers of lung cancer. As already discussed aldehydes in exhaled breath are

the most potential breath biomarkers of lung cancer. To this end different studies targeted at detecting different such aldehydes (1-nonanol, formaldehyde), long-alkyl-chain molecules, and benzene rings using SnO<sub>2</sub>, NiO, Co<sub>3</sub>O<sub>4</sub>, Cr<sub>2</sub>O<sub>3</sub>, CuO, and Mn<sub>3</sub>O<sub>4</sub> have been attempted. However, detection of lung cancer through exhaled gas analysis is much more difficult than detecting asthma, COPD, diabetes, hilatosis etc because there is no single biomarker for lung cancer. In this regard, scientists are trying to use arrays of non-specific sensors instead of specific sensors in an attempt to detect lung cancer by breath gas analysis. However, in this review we shall concentrate on the specific detection of breath biomarkers and thereby will not discuss any further in this regard.

#### **Major parameters influencing the sensing behaviour.—**

Morphology, size, and composition of nanomaterials play pivotal roles in determining key sensing parameters, such as, sensitivity, selectivity, and response/recovery time. Materials chemistry can be an effective tool in tailoring the shape, size, and composition of the nanomaterials. Figure 6 shows the basic parameters influencing sensing behavior.

**Major parameters affecting sensitivity.—**Gas/VOC sensing in semiconductor oxides is a surface phenomenon. Therefore, as surface to volume ratio (S/V) increases with decreasing particle

**Table V. Detection of H<sub>2</sub>S using semiconductor metal oxides.**

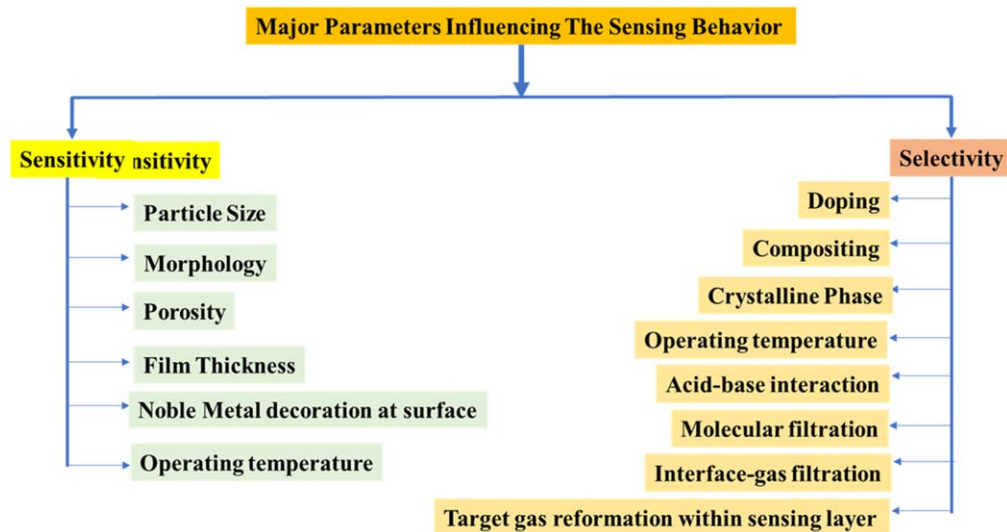
| Nanomaterial   | Morphology                        | Lowest concentration of H <sub>2</sub> S detected |
|--|-----------------------------------|---|
| CuO  | Nanowire                          | 10 ppb <sup>201</sup>                             |
| CuO  | Vertically aligned nanowire       | 500 ppb <sup>202</sup>                            |
| CuO  | Nanosheet                         | 2 ppb <sup>203</sup>                              |
| CuO  | Thin film                         | 100 ppb <sup>204</sup>                            |
| CuO  | Hierarchical hollow porous sphere | 2 ppb <sup>205</sup>                              |
| CuO-SnO <sub>2</sub>   | Thin film                         | 20 ppb <sup>206</sup>                             |
| Sb doped SnO <sub>2</sub>  | Nanoribbon                        | 100 ppb <sup>211</sup>                            |
| CuO loaded In <sub>2</sub> O <sub>3</sub>                          | Nanowire                          | 5 ppm <sup>212</sup>                              |
| CuO-ZnO  | Hollow sphere                     | 5 ppm <sup>213</sup>                              |
| Mo doped ZnO   | Nanowire                          | 5 ppm <sup>214</sup>                              |
| ZnO-MoO <sub>3</sub>   | Cage                              | 500 ppb <sup>215</sup>                            |
| ZnO  | Long chain of nanobeads           | 5 ppm <sup>216</sup>                              |
| ZnO  | Nanorod                           | 0.05 ppb <sup>217</sup>                           |
| MoO <sub>3</sub>   | Nanopaper                         | 0.25 ppm <sup>218</sup>                           |
| MoO <sub>3</sub> -Fe <sub>2</sub> (MoO <sub>4</sub> ) <sub>3</sub> | Core-shell                        | 1 ppm <sup>219</sup>                              |
| Mo doped SnO <sub>2</sub>  | nanoparticle                      | 0.25 ppm <sup>220</sup>                           |
| SnO <sub>2</sub> @Ag   | Yolk-shell                        | 5 ppm <sup>221</sup>                              |
| Ag doped TiO <sub>2</sub>  | Nanostructure                     | 1 ppm <sup>222</sup>                              |
| Ag doped $\alpha$ -Fe <sub>2</sub> O <sub>3</sub>                  | Nanostructure                     | 50 ppm <sup>223</sup>                             |
| $\alpha$ -Fe <sub>2</sub> O <sub>3</sub>                           | Hierarchical hollow nano-box      | 0.25 ppm <sup>224</sup>                           |
| $\alpha$ -Fe <sub>2</sub> O <sub>3</sub>                           | Nanochain                         | ppb level <sup>225</sup>                          |
| Au modified $\alpha$ -Fe <sub>2</sub> O <sub>3</sub>               | Thin film                         | ~10 ppm <sup>226</sup>                            |
| WO <sub>3</sub>  | Quantum dot                       | 20 ppb <sup>227</sup>                             |
| Pd functionalized WO <sub>3</sub>                                  | Porous nanostructure              | — <sup>228</sup>                                  |
| Au incorporated WO <sub>3</sub>                                    | Thin film                         | 100 ppb <sup>229</sup>                            |

size, sensitivity also increases. One of the methods of increasing S/V is to decrease the crystallite/particle size. For example, Xu et al.<sup>235</sup> showed that when the particle size of SnO<sub>2</sub> was reduced, the sensitivity towards CO and H<sub>2</sub> increased.

Another method of increasing surface area is by tailoring the particle morphology. 1-D structure, viz. nano-wire and nano-rods have the highest S/V. 2-D structures have relatively lower S/V and 3-D structures have the lowest S/V. Amongst 3-D structures sphere has the lowest S/V. Therefore, recently the thrust is on developing 1-D Nanomaterials. For example, Steinhauer et al.<sup>201</sup> developed CuO nanowires that could detect down to 10 ppb H<sub>2</sub>S. In another report Choi et al.<sup>161</sup> showed that Pt loaded porous WO<sub>3</sub> nanofiber could exhibit high sensitivity to 5 ppm acetone with a response of 28.9 [ $R_{air}/R_{gas}$ ]. Rout et al.<sup>112</sup> clearly showed that WO<sub>3</sub> nanowires have far

superior sensitivity with respect to WO<sub>3</sub> nanoplatelets (2-D structure) which again has higher sensitivity than spherical WO<sub>3</sub> nanoparticles, thereby proving the point again that enhanced S/V increases sensitivity.

As much as it is important to have high S/V, it is also of paramount importance that maximum available surface should be exposed to the target gas/VOC. For example, WO<sub>3</sub> based hierarchical structure with uniform mesopores of controlled sizes and interconnected channels were found to detect sub-ppm acetone.<sup>166</sup> Highly porous electrospun SnO<sub>2</sub> was found to have extremely high sensitivity ( $R_{air}/R_{gas} = 192$  at 5 ppm) to acetone.<sup>178</sup> Shin et al.<sup>179</sup> clearly showed the advantage of higher porosity by demonstrating that densely packed SnO<sub>2</sub> nanofibers had much inferior sensitivity as compared to assembled SnO<sub>2</sub> nanofibers with wrinkled layers and elongated channel like pores and voids.

**Figure 6.** Major parameters affecting sensing behavior.

Thickness of the sensing layer also affects the sensitivity of the sensor. Here also the same logics of S/V and surface area accessible to gas/VOC are applicable. As the sensing layer becomes progressively thinner, at some point of time it becomes thin film. A thin film is a virtually 2-D structure, whereas a thick film is a 3-D structure. Therefore, S/V ratio of thin film is much higher than thick film and hence in thin film sensitivity becomes higher. Also, in a thick film the inner part of the sensor coating is virtually inaccessible to the target gas/VOC. But in a thin film almost all the surface is available to the target gas. Therefore, absorption increases and also sensitivity. There have been multiple reports on thin film chemiresistors and their beneficial effects on sensitivity<sup>126–128,132,142,154,174,184,195,204,206,226,229,200</sup> and these have been discussed in necessary details in the previous part of this section.

Another interesting practice for increasing sensitivity is by decorating the oxide nanoparticles with noble metal nanoparticles. For example, Sen et al.<sup>167</sup> demonstrated that decorating  $\gamma$ -Fe<sub>2</sub>O<sub>3</sub> with Pt enhanced the nanomaterial's sensitivity and selectivity towards low ppm acetone. Pt functionalized WO<sub>3</sub> hemitube exhibited enhanced sensitivity to acetone ( $R_{\text{air}}/R_{\text{gas}} = 4.11$  at 2 ppm) with a detection lower limit of 120 ppb.<sup>160</sup> Pd functionalized WO<sub>3</sub> and Au incorporated WO<sub>3</sub> thin film demonstrated enhanced sensitivity towards H<sub>2</sub>S.<sup>228,229</sup>

Also, the working temperature should be as optimized. At very low temperatures there are not enough electrons in the conduction band and hence sensitivity will be low. On the other hand, at very high temperatures the desorption kinetics much surpasses the absorption kinetics, thereby reducing the sensitivity. Therefore, optimum operating temperature lies somewhere in between and this needs to be identified in each case. For room temperature sensors the band structure is manipulated such that there are enough electrons in the conduction band even at room temperature, thereby ensuring appreciable sensitivity at room temperature itself.

**Major parameters affecting selectivity.**—Other than sensitivity, selectivity is another important parameter of a gas sensor. Selectivity can be enhanced by few techniques, viz. doping the sensing material, changing the crystalline phase of the sensor material, and by varying the operating temperature. Humidity is one of the major cross-sensitive agents in case of breath analysis. Tricoli et al.<sup>236</sup> doped SnO<sub>2</sub> with 5% TiO<sub>2</sub> to reduce the cross-sensitivity to humidity and increased the sensitivity to ethanol. Si-stabilized flame-made  $\alpha$ -MoO<sub>3</sub> exhibited reduced sensitivity to even 90% humidity.<sup>134</sup> Similarly, Ti overlayer on MoO<sub>3</sub> thin films reduces cross-sensitivity towards carbon monoxide, sulphur dioxide, and hydrogen and increases sensitivity towards ammonia vapor.<sup>128</sup> rGO/WO<sub>3</sub> nanocomposite showed selective sensing towards 1.14 ppm ammonia even at 55% relative humidity.<sup>139</sup> Antimony trioxide (Sb<sub>2</sub>O<sub>3</sub>) doping in  $\gamma$ -Fe<sub>2</sub>O<sub>3</sub> reduced humidity sensitivity with respect to pristine  $\gamma$ -Fe<sub>2</sub>O<sub>3</sub>.<sup>167</sup> Myriads of other such example can be put forward. In this regard this should be mentioned that inspite of huge amount of research, the effect of doping and compositing on selective sensing of gas/VOCs is still highly empirical and unpredictable. One has to intuitively choose his dopant/ compositing material based on his work experience in the field and detailed knowledge of the prior art. To that end we have included a nearly exhaustive survey of oxides and their dopants/composites for sensitive and selective detection of major breath biomarker gases/VOCs (ref. sub-section "Semiconductor Oxides" and Tables II–V). However, in general it may be mentioned that generally transition metal oxides enhance selectivity and noble metal alloys decrease selectivity. However, noble metal alloys tend to increase selectivity.

It has been noted by some researchers that changing the crystalline phase might enhance selectivity towards a particular gas. For example,  $\epsilon$ -WO<sub>3</sub> has an affinity towards trace acetone.<sup>106,108</sup> Similar example is  $\gamma$ -Fe<sub>2</sub>O<sub>3</sub> which shows better affinity towards sub-ppm acetone as compared to  $\alpha$ -Fe<sub>2</sub>O<sub>3</sub>.<sup>167</sup>  $\alpha$ -MoO<sub>3</sub> exhibited is more selective to ammonia than the other crystalline phases of the same oxide.<sup>133</sup> Again, the choice of crystalline phase of oxide for the

selective detection of a particular gas/VOC is done purely based on the knowledge of prior art, experience in the field and by trial and error method.

There is another prominent factor that affects selectivity, viz. the operating temperature of the sensor. For example, NH<sub>3</sub> selectivity can be improved by selecting the operating temperature of 400 °C to 450 °C in  $\alpha$ -MoO<sub>3</sub>.<sup>127</sup> Selectivity towards sub-ppm acetone over humidity could also be increased by selecting an operating temperature of 300 °C.<sup>167</sup>

Further there are some other factors affecting selectivity. Cho et al.<sup>117</sup> reported that acid-base interaction between the acidic oxide of  $\alpha$ -MoO<sub>3</sub> and basic vapor of triethylamine is responsible for ultrasensitive (detection limit down to 45 ppb) and ultrasensitive (in presence of multiple other gases, such as, C<sub>2</sub>H<sub>5</sub>OH, CO, CH<sub>4</sub>, C<sub>3</sub>H<sub>8</sub>, H<sub>2</sub>, and NO<sub>2</sub>) detection of triethyl amine. Molecular filter may also increase selectivity. Sahm<sup>120</sup> et al. reported that the Pd doped and undoped SnO<sub>2</sub> sensor showed better selectivity towards methane (230 ppm) in presence of a molecular filter of Pd doped Al<sub>2</sub>O<sub>3</sub>. There are also some less practiced techniques described earlier in this section.<sup>118–120</sup>

**Semiconductor chalcogenides and C based semiconducting materials.**—Recently, these materials have spurred interest in researchers owing to their potential to detect breath biomarkers. However, the gas sensing behavior of these materials has not been studied that well until now. By far disilicides and diselenides of molybdenum and tungsten has been studied as gas sensors. The most probable sensing mechanism is the charge transfer reaction between the target analytes and the material. Although many literatures suggest that these materials exhibit p-type gas sensing behavior, it still remains elusive whether these materials are n-type or p-type semiconductors. However, these materials can detect both polar (ammonia and NO<sub>x</sub>) and non-polar (CO and methane) gases.<sup>237–239</sup> This is an advantage as compared to the CNT and rGO based gas sensors. These materials can not be used above 300 °C, for oxidative degradation starts near about that temperature. Nevertheless, these materials most certainly revealed themselves to be potential candidates for breath analysis sensors.

Carbon nanotube (CNT) has attracted huge attention since its discovery owing to its excellent physical and chemical properties, such as high surface to volume ratio and high surface activity.<sup>240,241</sup> CNT interacts with gas molecules at room temperature by charge transfer between gas/VOC molecules adsorbed at the surface and the CNT itself and acts like a p-type semiconductor.<sup>242</sup> The sensing properties of CNT depends on chirality, impurities, and defects in the structure.<sup>243,244</sup> It shows negligible interactions with the major breath gases, viz. nitrogen, oxygen, and water vapor. But it interacts well with other breath gases such as ammonia and NO<sub>x</sub>. Therefore, it seems to have great potential for breath analysis.

Graphene is another exotic functional material which might become useful in selective detection of breath biomarkers. Graphene has high surface to volume ratio and behaves like a p-type semiconductor. However, direct preparation of graphene is costly and hence in many cases it is prepared from graphene oxide by reduction (reduced graphene oxide, rGO). Pristine rGO can detect ammonia and NO<sub>x</sub><sup>245–247</sup> while rGO with functionally modified surface is known to detect other breath biomarkers, viz. acetone.<sup>248</sup>

CNTs, Graphene and semiconductor chalcogenides are potential candidates for the detection of ammonia and NO at lower temperatures than that of the oxides. Some of the important materials in this regard are MoS<sub>2</sub>,<sup>237</sup> electrokinetically fabricated CNT,<sup>249</sup> spin coated monolayer film of grapheme on interdigital electrodes,<sup>250</sup> cellulose derivative assisted dispersion of single-walled CNT (SWCNT),<sup>251</sup> ZnO functionalized graphene and MWCNT,<sup>159</sup> reverse-biased graphene/silicon heterojunction Schottky diode,<sup>252</sup> self-assembled r-GO nanosheets formed on high aspect ratio SU-8 micro-pillar arrays,<sup>253</sup> etc. Ng et al.<sup>254</sup> developed a nanocomposite gel comprised of uniform porous structure and a mixture of 3-D graphene material and an ionic liquid (1-butyl-3-methylimidazolium



hexafluorophosphate). The major advantage of using graphene, r-GO, SW- and MW-CNTs, and semiconductor chalcogenides lie in their low operating temperature and flexible structure.

**Electrochemical sensors.**—Use of electrochemical sensors for breath analysis to detect disease is a relatively novel field of research with much fewer reports with respect to that of semiconductor sensors. However, due to well-understood operating principle, high accuracy, low detection limits, wide-range of detection, biocompatibility, miniaturizability, low power consumption, and low cost the electrochemical sensors are gaining popularity amongst breath researchers. The few drawbacks of these sensors are long response time and inability to detect long chain VOCs. The enzyme based electrochemical sensors are highly selective, however, the non-enzymatic sensors suffer from cross-sensitivities from breath moisture and other competing VOCs/gases. The electrochemical cells that use aqueous electrolyte have to use gas permeable, hydrophobic membrane that allows the inward diffusion of gas but suppresses the outflow of water. Thus, the process becomes diffusion controlled and response time becomes very long. Multiple techniques have been adopted to solve this problem but the best solution is “fuel cell” technology that uses solid-electrolyte.

The most commonly detectable VOCs/gases by electrochemical technique are CO, NO, hydrogen peroxide, low chain-length aldehydes, and ethanol vapor. However, ethanol is not a breath biomarker for any disease or health condition. However, CO, NO and also hydrogen peroxide concentration in exhaled breath increase in case of airway inflammation, asthma, COPD, oxidative stress, lung cancer, and other such respiratory diseases. Therefore, the electrochemical detection of these biomarkers will be mostly discussed with one or two examples of breath alcohol analysis by electrochemical technique. The sole reason for including breath alcohol analysis is the fact that it is important for drunken driving testing. Already, BACtrack, a US based company has made fortunes making “fuel cell” based portable, commercial breath alcohol analyzers. There are very few reports on electrochemical detection of acetone in vapor phase for non-invasive detection of diabetes and ketosis. Those will also be discussed. Also, portable halimeters exploiting electrochemical methods are available commercially. A halimeter measures VSCs (Volatile Sulphur compounds, viz. hydrogen sulfide, methylmercaptan, other thiols, and dimethyl sulfide) for the detection of halitosis. The detection limits are as low as 5 ppb with response time of 1 s.<sup>255</sup> Further, there are electrochemical sensors that can detect ammonia from gas phase, but those were developed for air quality monitoring applications. Their specifications do not match well with the requirements of breath ammonia detection. Therefore, those discussions have been avoided in this review. However, interested readers may refer to the excellent review by R. Baron.<sup>256</sup>

A standard electrochemical sensor consists of a working electrode, a reference electrode, and a counter electrode. The gas/VOC passes through a permeable membrane and gets oxidized or reduced on the working electrode surface. The transfer of electrons that takes place as a result of the redox reaction flows from the working electrode through an external circuit and thereby generates the signal considered as the response of the electrochemical sensor. The purpose of the reference electrode is to indicate the potential of the electrolyte. The external circuit maintains the voltage across the working electrode and the reference electrode and also measures, amplifies, and processes the signal generated at the working electrode. Equal and opposite reaction occurs at the counter electrode, i.e., if oxidation takes place at the working electrode, reduction takes place at the counter electrode.

As has been already mentioned CO can be considered as a biomarker for hemolytic disease. However, fire fighters come across huge concentrations of CO while extinguishing big fires. Therefore, the content of carboxyhemoglobin increases in their blood which can lead to fatal conditions. During this period the exhaled breath CO

content also increases. It necessitates the development of a portable device using which the fire-fighter can measure his own breath CO content after extinguishing a fire and if the CO level in his breath is above the danger limit, he can seek immediate medical attention avoiding any casualty. In 1976, Stewart et al.<sup>257</sup> developed such an electrochemical device that can complete the measurement within 11–12 min in the real field.

Thereafter in 1994, Vreman et al.<sup>258</sup> reported the development of a device based on an amperometric electrochemical sensor for the detection of trace CO from exhaled breath. Reportedly, CO can be a biomarker for hemolytic disease. Platinum black coated Teflon was used as the working electrode. The performance of this device was found to be comparable with that of GC. In 2004, Hemmingsson et al.<sup>259</sup> reported the development of an amperometric electrochemical sensor based hand-held device for the real-time detection of NO from exhaled breath. The device was capable of detecting down to 3 ppb NO with a fast response time of 15 s only. The performance of this device was comparable with that of the FeNO testing considered as the gold standard for trace NO detection. Mondal et al.<sup>260</sup> developed a potentiometric electrochemical sensor for the detection of trace NO<sub>x</sub> from exhaled breath. They used a 2-electrode system, whereby the working electrode was fabricated by coating Pt wire with tungsten oxide (WO<sub>3</sub>) and the reference/counter electrode was fabricated by coating Pt loaded zeolite on Pt wire. Yttria stabilized zirconia (YSZ) was used as the solid electrolyte. Instead of a single sensor, an array of 20 sensors were used to increase the detection limit down to 5 ppb. The calibration of NO<sub>x</sub> with EMF was linear enough. Obermeier et al.<sup>261</sup> developed an electrochemical system to simultaneously detect CO, NO, and C<sub>1</sub>-C<sub>10</sub> aldehydes. The electrochemical sensors were amperometric in nature and were all procured from IT Dr Gamber GmbH Wismar, Germany (Dr Kerstin Wex). Both in vitro and in vivo measurements were conducted. The sensors were more sensitive than some chemoresistive sensors but lacked in selectivity. Hydrogen peroxide is known as a biomarker for oxidative stress. In patients with COPD, hydrogen peroxide content in exhaled breath increases. Therefore, monitoring of hydrogen peroxide in exhaled breath can reduce frequent hospitalization and exacerbation of the condition of the affected patient. To this end Wiedemair et al.<sup>262</sup> has developed a chip-integrated, amperometric, electrochemical sensor for the detection of trace hydrogen peroxide in exhaled breath. The working electrode was made of layers of Pt/Ta where Ta was used as the adhesion promoter with the substrate. The counter electrode was made of layers of Ag/Pd/Ti, where Ag is the electrode, Ti was the adhesion promoter and Pd acted as the diffusion barrier between Ti and Ag. The reference electrode was that of Ag/AgCl. Hydrogen peroxide was detected in both liquid phase and gaseous phase. However, in this review we are discussing about direct breath analysis in gaseous phase. For the gas phase measurement of hydrogen peroxide electrolyte with agarose gel dissolved in it was solidified on the electrodes. It was observed that with increasing concentration of hydrogen peroxide in the gaseous phase the current signal increases and the detection limit was estimated to approximately 42 ppb. 2-Butanone is known to be a biomarker for gastric cancer and can be detected in breath condensate.

Zhang et al.<sup>263</sup> reported the fabrication of an amperometric sensor for the detection of 2-butanone. They used an Au/Ag nanoparticle decorated MWCNT loaded glassy carbon electrode as the working one, a standard platinum wire as the counter electrode and a calomel electrode as the reference electrode. An aqueous solution of KCl was used as the electrolyte to which 2-butanone was dissolved and CV (cyclic voltammetry) study was conducted. The sensor showed high electrocatalytic activity to butanone and there was a linear relationship between the anodic peak current and the concentrations of 2-butanone in the range of 0.01% to 0.075%. Nitrite content in breath condensate was measured by Gholizadeh et al.<sup>264</sup> for point-of-care detection of chronic respiratory conditions such as, asthma and COPD. The primary source of this nitrite being NO in exhaled breath. As already



discussed, the concentration of NO in exhaled breath increases in respiratory inflammatory diseases, therefore, nitrite content should also increase in breath condensate. rGO coated gold electrode was used as the working electrode, Pt and Ag/AgCl were used as counter and reference electrodes, respectively. The sensitivity of the sensor was determined to be  $0.21 \mu\text{A} \mu\text{M}^{-1} \text{cm}^{-2}$  in the range of 20 to  $100 \mu\text{M}$  and  $0.1 \mu\text{A} \mu\text{M}^{-1} \text{cm}^{-2}$  in the range of 100 to  $1000 \mu\text{M}$ . The lowest detection limit was 830 nM. The results were comparable to the chemiluminescent devices. Mitsubayashi et al.<sup>265</sup> reported that they developed bioelectronic sniffer devices for detection of alcohol (1–100 ppm) and acetaldehyde (0.11–10 ppm) in exhaled breath using enzyme based electrochemical sensors. The alcohol sensor had a carbon electrode and an Ag/AgCl electrode and the enzyme used was alcohol oxidase. The acetaldehyde sensor had two Pt electrodes and the enzyme was aldehyde dehydrogenase. In both cases the change in current due to redox reaction at the working electrode was measured. Breath analysis of aldehyde is important for cancer detection, whereas detection of alcohol from exhaled breath is important for onsite detection of drunken driving.

Recently, Kawahara et al.<sup>266</sup> developed a chronoamperometric, chromatography paper based, enzymatic electrochemical sensor for the detection of ethanol vapor in the breath of an intoxicated person. The beauty of this device lied in the fact that the paper sensor was disposable, low cost, the power source was only a smart phone, and cost-effective graphite pencil was used to fabricate working and counter electrodes. In principle this technique can be used for any breath volatile/gas. Due to the enzymatic approach the selectivity of the sensor is unquestionable.

In the last few years, there have been two excellent reports on breath analysis by electrochemical methods for tuberculosis detection by D. Bhattacharya and Y R Smith. In 2016, Smith et al. reported<sup>267</sup> the detection of four tuberculosis (TB) biomarkers (VOBs), viz. methyl phenylacetate, methyl p-anisate, methyl nicotinate, and o-phenyl anisole by electrochemical methods. Cobalt functionalized titania nanotube array (TNA) produced by an incipient wetness method and insitu anodic oxidation method were used as functional materials. The insitu cobalt functionalized TNA (iCo-TNA) showed better response and selectivity to the TB biomarkers with concentrations ranging from 275–360 ppm. Later in 2016, Bhattacharya et al.<sup>268</sup> reported on the development of an electrochemical sensor for the detection of the same four VOBs of TB using a titania nanotube array (TNA) functionalized by Co by an incipient wetting impregnation (IWI) method. Here also, a two electrode amperometric sensing method was applied where the cobalt functionalized TNA was used as the working electrode. The sensors were able to detect low concentrations of the target analytes down to ~18 ppb. The enhanced sensitivity is attributed to the width of depletion layer that was comparable to half of the thickness of the TNA. As earlier the maximum sensitivity to methyl p-anisate was observed. The selectivity of the sensor to the TB biomarkers was also appreciable. The sensing platform is claimed to be robust, and inexpensive.

As already discussed, acetone is the breath biomarker of diabetes. Recently, some works related to electrochemical detection of trace acetone from exhaled breath has come forward. Martinez et al.<sup>269</sup> reported a PANI/Cellulose/ $\text{WO}_3$  based electrochemical sensor that is capable of detecting trace acetone in room temperature. The detection limit of the sensor was reported to be 10 ppm acetone in air. In another report Sorocki et al.<sup>270</sup> reported on a prototype, portable breath analyzer for exhaled acetone detection, the target application being point of care detection of type-1 diabetes. In their report there were no discussion on the functional material.

In brief, this is the current status of breath analysis by electrochemical methods. There are few other reports where electrochemical detectors are used in combination with analytical techniques, such as GC. These detectors can not be directly considered as sensors and are therefore left out of discussion in this review.

*Other potential nanomaterials.*—Scientists across the globe are constantly investing time, money, and tireless effort in design and development of new materials and techniques of detecting exhaled breath VOCs for the purpose of disease detection. Madasamy et al.<sup>271</sup> developed copper zinc superoxide dismutase (Cu, ZnSOD) that was immobilized on the carbon nanotubes in the polypyrrole modified platinum electrode and this was used as the NO biosensor. Poly (ethylene imine) coated carbon nanotube field effect transistor (NTFET) developed by Kuzmych et al.<sup>272</sup> The conductivity of the FET changed proportionally to the concentration of NO it was exposed to. Kao et al.<sup>273</sup> could detect down to 0.4 ppm acetone using an ultrathin (10nm) InN-FET. de Lacy et al.<sup>274</sup> developed a ppm/ppb level sensor for acetone, acetaldehyde, pentane and ethanol. The sensor was comprised of ultra violet light emitting diode activated zinc oxide nanoparticles that showed reversible resistance change when exposed to the said target VOCs. Gu et al.<sup>275</sup> fabricated Polyaniline/polystyrene single-nanowire based optical devices that were capable of detecting ammonia in ppm level.

Yebo et al.<sup>276</sup> demonstrated reversible ammonia sensing with ammonia-specific acidic nano-porous aluminosilicate film functionalized silicon-on-insulator optical micro-ring resonators. The detection limit was down to 5 ppm. Peng et al.<sup>277</sup> developed a random network of SWCNTs on an oxidized silicon wafer. This was further coated with 11 different non-polymeric organic materials (e.g. Dioctyl phthalate plasticizer, propyl gallate, anthracene etc) to develop an array of 11 sensors for differentiating individuals with lung cancer from healthy individuals. Peled et al.<sup>278</sup> used gold nanoparticles coated with 16 different non-polymeric organic materials (e.g. hexanethiol, 2-ethylhexanethiol, 3-methyl-1-butanethiol, octadecylamine, decanethiol etc.) to make an array of 16 non-specific sensors that could effectively differentiate between benign vs malignant pulmonary nodules, between adeno- and squamous-cell carcinomas, and between early stage and advanced stage of lung cancer disease. 72 patients were involved in the study.

Peng et al.<sup>279</sup> conducted a similar study with 177 volunteers in the age group of 20–75 years. Here the gold nanoparticles were functionalized by Dodecanethiol, 4-methoxy-toluenethiol, hexanethiol, 11-mercapto-1-undecanol, decanethiol, octadecanethiol etc (14 non-polymeric organic materials) to develop an array of 14 sensors that was used to detect different cancers, viz. lung, breast, colorectal, and prostate. Hakim et al.<sup>280</sup> diagnosed head and neck cancer from exhaled breath using an array of five sensors made of gold nanoparticles capped by tert-dodecanethiol, hexanethiol, 2-mercaptobenzoazole, 1-butanethiol, and 3-methyl-1-butanethiol ligands. In another work, Broza et al.<sup>281</sup> fabricated an array of 6 sensor prepared by coating organic ligands (11-mercaptoundecanol, oleylamine, dibutyl disulphide, decanethiol etc) on spherical gold nanoparticles and cubic platinum nanoparticles.

Chapman et al.<sup>282</sup> used a carbon polymer array (CPA) to differentiate patients of malignant mesothelioma from patients of asbestos-related disease and healthy individuals with an accuracy of 88%. Dragonieri et al.<sup>283</sup> used a similar kind of electronic nose to differentiate between malignant pleural mesothelioma and controlled healthy individuals. In another study, the author and his team fabricated an e-nose that could discriminate between non-small cell lung cancer and COPD.<sup>284</sup> Organic material coated carbon black and pristine carbon black were used as the functional materials for the sensors of the array. Xu et al.<sup>285</sup> diagnosed gastric cancer from benign gastric conditions using a nanomaterial-based sensor array containing 14 sensors. The sensors are composed of organic, non-polymer material (PAH5, PAH6, 2-ethylhexanethiol, tert-dodecanethiol etc) capped SWCNT and spherical gold nanoparticles. Timms et al.<sup>286</sup> used carbon black to detect gastroesophageal reflux disease from exhaled breath. Lonescu et al.<sup>287</sup> detected multiple sclerosis from exhaled breath using bilayers of polycyclic aromatic hydrocarbons (PAH1, PAH2, PAH6, PAH7) on SWCNT.

Tisch et al.<sup>288</sup> reported that Alzheimer's and Parkinson's disease can plausibly be detected from exhaled breath using SWCNT and spherical nanoparticles capped by 2-mercaptobenzoxazole, 3-mercaptopropionate,  $\beta$ -cyclodextrin etc. Shuster et al.<sup>289</sup> classified breast cancer precursors through exhaled breath analysis. The e-nose used consisted of an array of sensors comprised of organic non-polymer (benzyl mercaptan, calixarene, octadecylamine etc) coated cubic platinum nanoparticles. Lazar et al.<sup>290</sup> detected asthma from human exhaled breath using an array of 32 carbon black polymer sensors. Carbon black polymers were also employed by Fens et al.,<sup>291</sup> Chapman et al.,<sup>292</sup> and Biller et al.<sup>293</sup> for the detection of pulmonary embolism, obstructive sleep apnea, and airway inflammation, respectively.

Jalal<sup>294</sup> et al. reported to have developed a miniaturized fuel cell sensor based battery operated, wearable device that could detect the concentration of isoflurane (volatile anesthetic). The device is supposed to find application in safe transport of critically ill patients in austere conditions in unmanned drones. The electrodes were made of nickel-clad stainless steel and the solid electrolyte was poly-tetrafluoro-ethylene (PTFE) reinforced Nafion424. Ozhikandathi<sup>295</sup> developed a novel ninhydrin-PDMS composite to detect trace ammonia down to 2 ppm. The optical absorption property of the said composite changes when it is exposed to ammonia and that is the working principle of this sensor. Chung et al.<sup>296</sup> reported on a comparison of electrophoretically deposited (EPD) and drop coated hydrothermally synthesized NiO of multiple morphologies on a substrate. The EPD-NiO showed better sensitivity with respect to drop-coated NiO towards ethanol vapor for all morphologies. Ozdemir et al.<sup>297</sup> compared the NO sensitivities of naked porous silicon (PS) and SnO<sub>2</sub> modified PS. It was reported that SnO<sub>2</sub> decorated PS showed much better (10 times higher) response than naked PS at 1 ppm NO exposure. Detection of asthma from exhaled breath was put forward as a plausible application of this sensor.

Therefore, it is clear that non-specific sensor arrays can effectively detect diseases that are difficult to be detected by specific sensors. The general strategy of making such sensors would be to coat functional organic non-polymeric materials on nanoparticles of noble materials (e.g. Au, Pt etc), SWCNT or carbon black. Additionally some fantastic nanomaterials in the field of electrochemical gas sensors are coming up. This opens up new avenues towards the detection of diseases from exhaled breath analysis.

**Other techniques.**—Alongside the techniques discussed above there are few more techniques that have come in vogue in recent times. Although the focus of this review is not on these techniques, still we will discuss some of these techniques in brief for completeness and to enhance the appeal of this review to a broader readership.

**Nanomaterial based field effect transistor (FET).**—These materials have advantages over the existing semiconductor gas sensors in regards, such as extreme miniaturizable features, low-power consumption and appreciable control over the sensor signals by controlling the source-gate potential. Shehada et al.<sup>298</sup> used modified Silicon nanowire FETs to detect gastric cancer. Kao et al.<sup>299</sup> used an ultrathin InN FET to detect sub-ppm acetone.

**Colorimetric sensors.**—As evident from the name colorimetric sensors change color in presence of the target VOCs and the degree of change in color should be related with the concentration of the VOC. Mazonne et al.<sup>300,301</sup> showed that various types of lung cancers can be detected using an array of colorimetric sensors with reasonably good accuracy (for e.g. 81.1%). Alagirisamy et al.<sup>302</sup> used an iodine solution and starch to detect down to 0.05  $\mu\text{g l}^{-1}$  hydrogen sulphide. The authors demonstrated good correlation between the volatile sulfur compounds (VSC) detected by the developed sensor and halimeter. This study was important for the detection of breath malodor and halitosis from exhaled breath.

**Piezoelectric sensor.**—It works in conjunction with a quartz crystal microbalance (QCM). The oscillation frequency of QCM changes when it absorbs VOCs and a piezoelectric sensor measures that change. The surface absorption of gases on QCM can be controlled by coating it with various polymers, metal oxides, nanomaterials etc. Lung cancer, COPD, Asthma, and Halitosis was reported to be detected from breath samples by metalloporphyrin-based QMB sensors<sup>303–307</sup> by D'Amico et al., Natale et al., Incalzi et al., Montuschi et al., and Pennazza et al.

**Surface acoustic wave (SAW) sensor.**—This is a class of sensor based on microelectromechanical systems (MEMS). It converts an input electrical signal into a surface acoustic wave, i.e. a mechanical wave. Unlike the electrical signal the mechanical wave can be easily influenced by the physical phenomena. The modulated SAW is then again converted into an electrical signal that is received at the output end. The changes in amplitude, phase, frequency, or time-delay between the input and output signal can be used to measure any physical phenomenon that might have affected the wave. SAW sensors are coated with various polymers to detect different breath biomarkers and hence various diseases from the exhaled breath. For example, SAW sensors have been used to detect lung diseases,<sup>308</sup> pulmonary tuberculosis<sup>309</sup> etc.

**Optical fiber based sensors.**—In recent times, Optical fiber based gas sensors have come up in such a big way that a separate review can be written only on this subject. However, here we will merely scratch the surface of what it is. A small part of the cladding is removed and coated with polymer, chemical dye, oxides etc in the form of thin films and when this layer absorbs VOCs, that triggers a change in the refractive index or other transmission properties. Although, different VOCs have been detected using these sorts of sensors, there is by far no report of real exhaled breath analysis using such sensors.

**Laser photoacoustic spectroscopy (LPAS).**—Carbon dioxide laser is used for this purpose. The laser excites sample gas inside a photoacoustic cell. The photoacoustic signals are proportional to the trace gas concentration. The LPAS has been reported to have been capable of detecting down to 0.2 ppb of ethylene in nitrogen at 1 atm pressure.<sup>310</sup>

**Chemiluminescence analyzer.**—Chemiluminescence is the standard technique of measuring NO. These sensors are very sensitive and can detect down to ppb-level. It can therefore be used for the detection of asthma from exhaled breath. However, the system is bulky, costly and suffers from drift that needs to be corrected at least once in a year. This limits its use for home monitoring.

## Assessment of Exposure to VOCs

**Occupational and non-occupational exposure.**—Before 2000, employees in petroleum-related industries were considered to be at risk due to potentially hazardous VOCs. Now few other occupations are also in that list, viz. traffic policeman, service station attendants, parking garage attendants, and road side/ underground storekeepers.<sup>311</sup> Benzene, a group I carcinogen, is used as a common solvent in production of petrochemical and pharmaceutical goods, pesticides, synthetic dyes etc. Therefore, people working there fall victims to the carcinogenic effects of benzene. It has been established that exhaled breath analysis can be used to differentiate biological benzene levels in healthy individuals from the occupationally exposed individuals 16 h after the end of their working shift.<sup>312</sup> However, smokers have higher benzene levels in breath than normal individuals and hence proper measures should be taken for accurate measurements of occupational benzene levels in their breaths. Some other major aromatic compounds related to occupational exposure are, toluene, xylene and ethylbenzene. Toluene and xylene are found in excess in exhaled breath of house and car painters, varnish workers. Excess of Ethylbenzene and

xylene are found in the exhaled breath of dry cleaners. BTEX (Benzene, toluene, ethylbenzene and xylene) analysis of exhaled breath can be used as a measure of occupational VOC hazard. Other such VOCs are trimethylbenzene, naphthalene, tetrachloroethane, isoflurane etc.

Asbestos is another occupational peril. Although, Asbestos is not a VOC, airborne fine asbestos fibers easily get to the lower portion of lungs with inhaled breath and cause potentially fatal diseases. People working in asbestos mining, processing of asbestos mineral, construction works, mechanics of vehicles, insulation workers in the heating trade, sheet metal workers, plumbers, fitters, cement and custodial workers etc are at risk of falling prey to asbestosis (a fibrotic disease), MPM (Malignant Pleural Mesothelioma, caused by change in the pleural lining), and lung cancer. Biomarkers such as NO, 8-isoprostane, leukotriene B<sub>4</sub>,  $\alpha$ -Pinene (asbestosis) and cyclohexane (MPM) have been identified as breath biomarkers. By far there is no blood test for early detection of MPM. Therefore, breath analysis may have massive impact in the early detection of asbestos related diseases.

Rapid industrialization, increased traffic volumes, increased use of pesticides and synthetic materials etc have elevated the air pollution level to an unforeseen level. Therefore, non-occupational exposure to different VOCs are posing major threats to human health. Most of such VOCs are easily carried to the lungs through inhaled breath and readily absorbed in blood. Therefore, their presence in exhaled breath also increases. NO, SO<sub>x</sub>, ammonia, alkanes, halogenated compounds, ketones, aromatic hydrocarbons, terpenes, various alcohols, toluene, xylene etc are some of the major pollutants causing health hazards. As already discussed in previous sections, various studies are going on to detect such volatiles from exhaled breath.

### Parameters Affecting VOCs Levels

Other than endogenous processes there are multiple other parameters that affect the VOC levels measured in the exhaled breath.

**Exogenous origin.**—As discussed in the previous section VOCs such as, NO, NH<sub>3</sub>, benzene etc could be of both exogenous and endogenous origin. These could be inhaled or absorbed through skin. Therefore, the concentration of such VOCs in exhaled breath does not necessarily reflect the health conditions. Also, search for new biomarkers are in vogue. Many of the exhaled VOCs are absolutely exogenous in origin. It is therefore important to differentiate between exogenous and endogenous VOCs, so that an exogenous VOC does not wrongly get identified as a biomarker. Background VOC is an issue. It is generally considered that when inhaled concentrations of compounds are greater than 5% of the exhaled concentrations, exhaled breath concentrations can not be correlated to blood VOC concentrations with confidence.

**Mouth vs nose exhaled breath.**—Exhaled breath analysis is mostly focused on mouth exhaled breath. However, other than VOCs of systemic origin, mouth exhaled breath contains VOCs originating from the airway, from oral cavity and gut by bacterial action, from mucus and saliva. This makes disease detection and health monitoring from exhaled breath difficult. Wang et al.<sup>313</sup> compared exhaled breath from mouth, nose and air in mouth cavity. It was observed that acetone and isoprene are absolutely systemic in origin. Other VOCs, viz. ammonia, hydrogen sulphide, and ethanol are mostly mouth-generated. Methanol, propanol and other VOCs have partly systemic origins. Although concentration of VOCs exhaled from nose have lower concentrations than those in breath, but it obviates the confounding factors present in the mouth exhaled breath. Therefore, nose exhaled breath analysis might be more desirable.

**Alveolar breath vs dead space air.**—The exhaled breath is a combination of dead space air and alveolar air. Dead space air is

defined as the volume of air that acts as a conducting path and alveolar air exchanges VOCs with blood. and VOCs in alveolar breath is supposed to be in equilibrium with the VOCs in blood. It is therefore desirable to measure the alveolar breath. The last fraction of exhaled breath, known as the end tidal breath is close in composition with the alveolar breath.

**Dilution of highly water soluble VOCs.**—Measurement of less soluble VOCs from exhaled breath is easier. However, for highly soluble VOCs, such as acetone and isoprene such measurement becomes difficult as an anatomic dead-space cannot be defined for such compounds. Most of the exchange of such VOCs occurs at the airway rather than at the alveoli. During inspiration soluble gases are absorbed by the inhaled air in the airway. When it reaches the alveoli, the air is already saturated in soluble gases and no more exchange occurs. During expiration a part of the solubilised gas is re-dissolved in the mucus layer coating the airway. Thus, on the way up the respiratory tract the soluble gases get diluted. Also, an increased blood flow reduces the soluble gas concentration in exhaled breath. It is therefore suggested that holding the breath for 10 s before exhalation may result in more accurate results in exhaled breath analysis.

**Influence of age, gender, food and pregnancy.**—Isoprene is much less in the breath of children as compared to the adults. At puberty the isoprene concentration is elevated.<sup>314,315</sup> Also, several studies suggest that isoprene concentration in males is more than the females.<sup>316</sup> Further, there are reports of increasing ammonia concentration with age.<sup>22</sup> Clearly, age and gender influence the VOC content in exhaled breath.

It is well-known that intoxication increases exhaled breath ethanol concentration. Also, intake of garlic, onion, mint, banana, coffee, orange, flavoured ice-cream etc are known to change the exhaled breath composition.

Pregnancy in women affects their exhaled breath composition, however no concrete relationship has yet been found.

**Influence of storage conditions.**—Direct analysis is preferable over storage of breath samples. However, not all breath analysis techniques support direct analysis. Storage should be done with utmost care in order to avoid loss of breath components due to diffusion, background emission of pollutants, VOC influx from the storage container, degradation of the sample by reaction of sample container with the breath VOCs etc. Currently, the most popular way of storing breath is in Tedlar bags. Other materials are Flexfoil bags, Nalophan bags, micropacked sorbent traps, glass vials (SPME), metal canisters etc.

### Challenges

Detection of disease and monitoring of health through blood analysis are invasive and painful processes. In the recent past exhaled breath analysis has emerged as a better alternative, mostly because of its non-invasive nature. However, the method is fraught with multiple challenges.

- GC-MS, PTR-MS and SIFT-MS are by far the most accurate techniques for breath analysis. But, these instruments are costly, cumbersome and need trained person for handling, data analysis and data interpretation. These instruments are not like any household devices and can only be available in hospitals and diagnostic clinics. This impedes the use of these instruments as breath analysers on a day to day basis at our homes. One of the major goals of breath analysis is early detection of disease by regular health monitoring and for that to be possible the device used must be financially affordable for common man, easy to use even for a layman and hand held.
- Not all the breath analysis techniques can make use of direct exhaled breath. Breath collection and storage therefore, becomes a

major issue. Collected breath that was stored for a long time often tends to degrade changing their original composition. Also, researchers are still not sure whether nose-exhaled or mouth-exhaled breath should be used for analysis. Even there are disputes regarding testing single and multiple breath. Now a days it is suggested that dead space air should not be considered for analysis, only end-tidal breath should be used. However, for highly water-soluble breath biomarkers, viz. acetone and isoprene there is no anatomic dead space that can be defined. Also, most of the sensor responses are dependent on the exhaled-breath flow-rate onto the sensor head. In direct analysis, patients directly blow on to the sensor head. However, different patients would blow at different flow-speeds, therefore making the measurement complicated. Also, exhaled breath concentration of different gases varies significantly with age, gender, weight, food habits, life style, pregnancy etc. Also, not all the exhaled breath components are endogenous, rather most are exogenous in origin. Many of the endogenous gases are not even systemic in origin. Therefore, locality becomes another confounding factor.

- Semiconductor oxide sensors are cost-effective, rugged, easy-to-use, and handy. They are capable of detecting different breath biomarkers at ppm, ppb or even ppt levels. However, these sensors, in most cases, lack sufficient specificity. Another major problem with these sensors is that they are mostly sensitive to humidity. Human breath contains almost saturated moisture which acts as a major cross-sensitive agent impeding the response of the sensor to target analyte. Presently thick film semiconductor oxide sensors are available in the market. Thick film sensors suffer from lower sensitivity, and high power consumption. Further, their relatively bigger sizes do not allow the integration of multiple such sensors in the form of a sensor array in a single device of reasonably small size to do away with the specificity problem. MEMS based sensor arrays can address the problem of size and power to some extent however, they have other problems. Microsystems generally use moisture traps, which along with moisture adsorbs analyte gases too. Humidity dependence of gas adsorption can significantly reduce the reliability and reproducibility of the preconcentrator. Also, preconcentration requires longer time; thereby making real-time analysis difficult. Further, the small volume of preconcentrator materials present in such microsystem might not be sufficient for detection of trace gases. Also, selective and reversible preconcentration remain challenges.

- Graphene and CNT based materials, FET, Laser, SAW, colorimetry and optical fibre-based sensors are emerging as novel materials and techniques, however, these are far from commercialization.

- In recent times electrochemical sensors have drawn attention of breath researchers owing to well-understood operating principle, high accuracy, low detection limits, wide-range of detection, biocompatibility, miniaturizability, low power consumption, and low cost. However, the technique is not without a few drawbacks, viz. long response time and inability to detect long chain VOCs.

- Specific sensors for the detection of diseases from exhaled breath is limited to a small number of diseases, such as, diabetes, COPD etc which can be detected using a single biomarker. In most of the diseases, especially different cancers, concentrations of multiple breath gases change simultaneously. This is a difficult problem to be handled using specific sensors. Also, use of specific sensors demand the development of highly selective nanomaterials. This is a paramount challenge in itself. Non-specific sensors can obviate the problems encountered by specific sensors; however, these sensors suffer from low to medium sensitivity. Therefore, obtaining sufficient discrimination between diseased and healthy group might become difficult.

It is therefore clear that in spite of all the prospects that breath analysis brings to the table, developing successful, commercial breath-analysers is fraught with multiple challenges that the researchers world-wide are trying to mitigate.

## Potential and Plausible Future of Breath Research

It is beyond doubt that in the near future breath analysis will at least complement if not replace blood-analysis for disease detection. For example, BACtrack is selling “solid oxide fuel cell” based portable breath alcohol analyzer for drunken driving test for 15 years now. Portable halimeters measuring VSCs (Volatile Sulphur compounds, viz. hydrogen sulfide, methylmercaptan, other thiols, and dimethyl sulfide) for the detection of halitosis are available commercially. Portable electrochemical sensor for the detection of trace acetone in exhaled breath is also reported. BOSCH Healthcare Solutions<sup>®</sup> have already proposed a hand-held breath analyzer for the detection of asthma from exhaled breath. Peak flow meter is a standard technique for the detection of asthma, COPD and other breathing troubles causing shortness of breath.

Dr P. Gouma has demonstrated a diabetic breath analyzer prototype. Ronnie Priefer and Michel Rust, of Western New England University, Springfield, MA and Christine Sleppy, of University of Central Florida have developed similar working prototype diabetic breath analysers. Robert Peverall et al. has also come up with a breath acetone detector that uses sample preconcentration and cavity enhanced spectroscopy. However, breath analysis for disease detection is still in its infancy. The future of breath research should be targeted on

- Discovering new biomarkers or set of biomarkers,
- Establishing standard correlations between blood and exhaled breath concentrations of biomarkers, Establishing standard breath collection and storage procedures,
- Differentiating between exogenous and endogenous gases in exhaled breath,
- Developing novel specific nanomaterials for selective detection of breath gases,
- Developing MEMS based miniaturized, portable, low-power devices that use novel, non-specific sensors,
- Reducing the effect of humidity on the sensors,
- Developing simple, repeatable, reproducible, reliable, real-time, light-weight, hand held devices that would be inexpensive,
- Fabricating wearable devices and integrating the technology with Internet of Things (IoT) using preferably smart-phone based applications,
- Reducing the power consumption to such low levels that body-heat, simple exercise or even walking can recharge the battery of the wearable device,
- Proper clinical trial including as many subjects as possible and validation of the prototypes,

On the basis of the above requirements, it seems that the way ahead requires a synergistic endeavor involving researchers of multiple disciplines, such as material researchers, MEMS fabrication specialists, electronics and instrumentation specialists, IoT specialists, and medical doctors.

## Conclusions

In conclusion, breath analysis is an interdisciplinary field of research work which includes medical science, analytical techniques, materials chemistry, data processing and electronics. It is a rapidly growing field which can tremendously contribute to the society by early detection of diseases. There exist devices which can be utilized for breath analysis; however, they are bulky, needs trained manpower, costly and not suitable for day to day use. Monitoring of diseases and assessment of exposure to VOCs/gases by analysing exhaled breath using a breathalyzer still has lot of challenges to overcome which includes standardization, sampling methods, defining markers. In particular, moisture of exhaled breath is an important interfering agent which contributes to sensing and produce erroneous results. A standard, robust and cheap breath-analyzer can come to market for day to day use only when all issues will be resolved.



## Acknowledgment

The authors are thankful to Dr Somnath Bandyopadhyay, Sr Principal Scientist & Head, Functional Materials and Devices Division, CSIR-Central Glass and Ceramic Research Institute, Kolkata for his moral support. The authors are also thankful to the Dr K Muraleedharan, Director, CSIR-Central Glass and Ceramic Research Institute, Kolkata for his kind support.

## References

1. T. H. Risby, A. Amann, and D. Smith, "Current status of clinical breath analysis," in *Breath Gas Analysis for Clinical Diagnosis and Therapeutic Monitoring*, ed. A. Amann and D. Smith (World Scientific, Singapore) p. 251 (2005).
2. T. H. Risby and S. F. Solga, "Current status of clinical breath analysis," *Appl. Phys. B*, **85**, 421 (2006).
3. T. H. Risby and F. K. Tittel, "Current status of midinfrared quantum and interband cascade lasers for clinical breath analysis," *Opt. Eng.*, **49**, 111123 (2010).
4. A. G. Dent, T. G. Sutedja, and P. V. Zimmerman, "Exhaled breath analysis for lung cancer," *J. Thoracic Dis.*, **5**, S540 (2013).
5. L. Pauling, A. B. Robinson, R. Teranishi, and P. Cary, "Quantitative analysis of urine vapor and breath by gas-liquid partition chromatography," *Proc. Natl. Acad. Sci.*, **68**, 2374 (1971).
6. M. Phillips, K. Gleeson, J. M. B. Hughes, J. Greenberg, R. N. Cataneo, L. Baker, and W. P. McVay, "Volatile organic compounds in breath as markers of lung cancer: a cross-sectional study," *Lancet*, **353**, 1930 (1999).
7. T. A. Popov, "Human exhaled breath analysis," *Ann. Allergy Asthma Immunol.*, **106**, 451 (2011).
8. T. Hibbard and A. J. Killard, "Breath ammonia analysis: clinical application and measurement," *Breath Ammon. Clin. App. Meas.*, **41**, 21 (2011).
9. W. Lindinger and A. Hansel, "Analysis of trace gases at ppb levels by proton transfer reaction mass spectrometry (PTR-MS)," *Plasma Sources Sci. Technol.*, **6**, 111 (1997).
10. M. Murtz, "Breath diagnostics using laser spectroscopy," *Opt. Photonics News*, **16**, 30 (2005).
11. W. Lindinger, A. Hansel, and A. Jordan, "On-line monitoring of volatile organic compounds at ppt levels by means of proton-transfer-reaction mass spectrometry (PTR-MS) medical applications, food control and environmental research," *J. Mass Spect. Ion Proc.*, **173**, 191 (1998).
12. C. Warneke, J. Kuczynski, A. Hansel, A. Jordan, W. Vogel, and W. Lindinger, "Proton transfer reaction mass spectrometry (PTR-MS): propanol in human breath," *J. Mass Spect. Ion Proc.*, **154**, 61 (1996).
13. Z. Wang and C. Wang, "Is breath acetone a biomarker of diabetes? A historical review on breath acetone measurements," *J. Breath Res.*, **7**, 037109 (2013).
14. A. Bajtarevic, C. Ager, M. Pienz, M. Klieber, K. Schwarz, M. Ligor, T. Ligor, W. Filipiak, H. Denz, and M. Fiegl, "Noninvasive detection of lung cancer by analysis of exhaled breath," *BMC Cancer*, **9**, 1 (2009).
15. B. Buszewski, M. Keszy, T. Ligor, and A. Amann, "Human exhaled air analytics: biomarkers of diseases," *Biomed. Chromatogr.*, **21**, 553 (2007).
16. J. Shaji and D. Jadhav, "Breath biomarker for clinical diagnosis and different analysis technique," *Res. J. Pharm. Biol. Chem. Sci.*, **1**, 639 (2010).
17. D. Smith, C. Turner, and P. Španěl, "Volatile metabolites in the exhaled breath of healthy volunteers: their levels and distributions," *J. Breath Res.*, **1**, 014004 (2007).
18. B. Buszewski, M. Keszy, T. Ligor, and A. Amann, "Human exhaled air analytics: Biomarkers of diseases," *Biomed. Chromatogr.*, **21**, 553 (2007).
19. W. Miekiš, J. K. Schubert, and G. Noeldge-Schomburg, "Diagnostic potential of breath analysis—focus on volatile organic compounds," *Clin. Chim. Acta*, **347**, 25 (2004).
20. C. Turner, P. Španěl, and D. Smith, "A longitudinal study of methanol in the exhaled breath of 30 healthy volunteers using selected ion flow tube mass spectrometry," *SIFT-MS. Physiol. Meas.*, **27**, 637 (2006).
21. J. Taucher, A. Hansel, A. Jordan, R. Fall, J. H. Futrell, and W. Lindinger, "Detection of isoprene in expired air from human subjects using proton-transfer-reaction mass spectrometry," *Rapid Commun. Mass Spectrom.*, **11**, 1230 (1997).
22. P. Španěl, K. Dryahina, and D. Smith, "Acetone, ammonia and hydrogen cyanide in exhaled breath of several volunteers aged 4–83 years," *J. Breath Res.*, **1**, 011001 (2007).
23. P. Španěl and D. Smith, "Selected ion flow tube," *Rapid Commun. Mass Spectrom.*, **13**, 585 (1999).
24. A. M. Diskin, P. Španěl, and D. Smith, "Increase of acetone and ammonia in urine headspace and breath during ovulation quantified using selected ion flow tube mass spectrometry," *Physiol. Meas.*, **24**, 191 (2003).
25. M. Righettoni, A. Amann, and S. E. Pratsinis, "Breath analysis by nanostructured metal oxides as chemo-resistive gas sensors," *Mater. Today*, **18**, 163 (2015).
26. J. M. Berg, J. L. Tymoczko, and L. Stryer, "Protein turnover and amino acid catabolism," in *Biochemistry* (W H Freeman, New York, NY) 5th ed., p. 633 (2002).
27. D. Voet, J. G. Voet, and C. A. Pratt, "The urea cycle," in *Fundamentals of Biochemistry* (Wiley, New York, NY) p. 620 (1999).
28. P. Tate, "Protein metabolism," in *Seeley's Principles of Anatomy and Physiology* (McGraw-Hill Companies, Inc., New York, NY) p. 704 (2009).
29. I. O. Essiet, "Diagnosis of kidney failure by analysis of the concentration of ammonia in exhaled human breath," *J. Emerg. Trends Eng. Appl. Sci.*, **4**, 859 (2013).
30. R. F. Butterworth, "Hepatic encephalopathy," *Alcohol Res. Health*, **27**, 240 (2003).
31. National Digestive Diseases Clearing House, Available online: <http://digestive.niddk.nih.gov/diseases/pubs/hpylori/index.htm> (accessed: December 17, 2014).
32. D. J. Kearney, T. Hubbard, and D. Putnam, "Breath ammonia measurement in *Helicobacter pylori* infection," *Dig. Dis. Sci.*, **47**, 25232 (2002).
33. A. Amano, "Monitoring ammonia to assess halitosis," *Oral Surg. Oral Med. Oral Pathol.*, **94**, 692 (2002).
34. A. M. Van den Broek, L. Feenstra, and C. de Baat, "A review of the current literature on aetiology and measurement methods of halitosis," *J. Dent.*, **35**, 627 (2007).
35. G. MacGregor, "Breath condensate ammonium is lower in children with chronic asthma," *Eur. Respir. J.*, **26**, 271 (2005).
36. S. Moncada and A. Higgs, "The L-arginine-nitric oxide pathway," *New Engl. J. Med.*, **329**, 2002 (1993).
37. C. Nathan, "Nitric oxide as a secretory product of mammalian cells," *FASEB J.*, **6**, 3051 (1992).
38. I. D. Pavord, D. E. Shaw, P. G. Gibson, and D. R. Taylor, "Inflammometry to assess airway diseases," *Lancet*, **372**, 1017 (2008).
39. S. A. Kharitonov, D. Yates, and P. J. Barnes, "Increased nitric oxide in exhaled air of normal human subjects with upper respiratory tract infections," *Eur. Respir. J.*, **8**, 295 (1995).
40. P. J. Barnes and S. A. Kharitonov, "Exhaled nitric oxide: a new lung function test," *Thorax*, **51**, 233 (1996).
41. W. Maziak, S. Loukides, S. Culpitt, P. Sullivan, S. A. Kharitonov, and P. J. Barnes, "Exhaled nitric oxide in chronic obstructive pulmonary disease," *Am. J. Respir. Crit. Care Med.*, **157**, 998 (1998).
42. J. Dotsch, S. Demirakca, H. G. Terbrack, G. Huls, W. Rascher, and P. G. Kuhl, "Airway nitric oxide in asthmatic children and patients with cystic fibrosis," *Eur. Respir. J.*, **9**, 2537 (1996).
43. R. Wang, "Two's company, three's a crowd: can H<sub>2</sub>S be the third endogenous gaseous transmitter?" *FASEB J.*, **16**, 1792 (2002).
44. E. Lowicka and J. Beltowski, "Hydrogen sulfide (H<sub>2</sub>S)—the third gas of interest for pharmacologists," *Pharmacol. Rep.*, **59**, 4 (2007).
45. O. A. Miasoedova and V. I. Korzhov, "Role of hydrogen sulfide in the realization of organism's physiological functions," *J. NAMS Ukraine*, **17**, 191 (2011).
46. M. M. Gadalla and S. H. Snyder, "Hydrogen sulfide as a gasotransmitter," *J. Neurochem.*, **113**, 14 (2010).
47. H. Kimura, "Hydrogen sulfide: its production and functions," *Exp. Physiol.*, **96**, 833 (2011).
48. J. F. Wang, Y. Li, J. N. Song, and H. G. Pang, "Role of hydrogen sulfide in secondary neuronal injury," *Neurochem. Int.*, **64**, 37 (2014).
49. C. F. Toombs, M. A. Insko, E. A. Wintner, T. L. Deckwerth, H. Usansky, K. Jamil, B. Goldstein, M. Cooreman, and C. Szabo, "Detection of exhaled hydrogen," *Br. J. Clin. Pharmacol.*, **69**, 626 (2010).
50. M. Rosenberg and C. A. McCulloch, "Measurement of oral malodor: current methods and future prospects," *J. Periodontol.*, **63**, 776 (1992).
51. F. L. Suarez, K. J. Furne, J. Springfield, and D. M. Levitt, "Morning breath odor: Influence of treatments on sulfur gases," *J. Dent. Res.*, **79**, 1773 (2000).
52. M. Rosenberg, "Clinical assessment of bad breath: current concepts," *J. Am. Dent. Assoc.*, **127**, 475 (1996).
53. A. Nilsson, Development of a handheld meter for monitoring of diabetes using exhaled air (accessed: December 17, 2014), [http://tekniskdesign.se/download/Rapport\\_Exjobb\\_-\\_AndersNilsson\\_-\\_INLAGA.pdf](http://tekniskdesign.se/download/Rapport_Exjobb_-_AndersNilsson_-_INLAGA.pdf).
54. O. B. Crofford, R. E. Mallard, R. E. Winton, N. L. Rogers, C. Jackson, and U. Keller, "Acetone in breath and blood," *Trans. Am. Clin. Climatol. Assoc.*, **88**, 128 (1977).
55. S. Massick, in *Portable Breath Acetone Measurements Combine Chemistry and Spectroscopy* (Southwest Sciences, Inc., Santa Fe, NM, USA) p. 1 (2007).
56. T. Toyooka, S. Hiyama, and Y. Yamada, "A prototype portable breath acetone analyzer for monitoring fat loss," *J. Breath Res.*, **7**, 036005 (2013).
57. J. Yang, Q. Nie, H. Liu, M. Xian, and H. Liu, "A novel MVA-mediated pathway for isoprene production in engineered *E. coli*," *BMC Biotech.*, **16**, 5 (2016).
58. L. T. McGrath, R. Patrick, and B. Silke, "Breath isoprene in patients with heart failure," *Eur. J. Heart Fail.*, **3**, 423 (2001).
59. C. A. Riely, G. Cohen, and M. Lieberman, "Ethane evolution: a new index of lipid peroxidation," *Science*, **183**, 208 (1974).
60. L. Breiman, "Random forests," *Mach. Learn.*, **45**, 5 (2001).
61. B. Efron, "Bootstrap methods: another look at the jackknife," *Ann. Stat.*, **7**, 1 (1979).
62. P. J. Mazzone, J. Hammel, R. Dweik, J. Na, C. Czich, D. Laskowski, and T. Mekhail, "Diagnosis of lung cancer by the analysis of exhaled breath with a colorimetric sensor array," *Thorax*, **62**, 565 (2007).
63. J. Shawe-Taylor and N. Cristianini, in *Kernel Methods for Pattern Analysis* (Cambridge University Press, Cambridge) (2004).
64. P. Paredi, S. A. Kharitonov, D. Leak, S. Ward, D. Cramer, and P. J. Barnes, "Exhaled ethane, a marker of lipid peroxidation, is elevated in chronic obstructive pulmonary disease," *Am. J. Respir. Crit. Care Med.*, **162**, 369 (2000).
65. M. D. Knutson, G. J. Handelman, and F. E. Viteri, "Methods for measuring ethane and pentane in expired air from rats and humans," *Free Radic. Biol. Med.*, **28**, 514 (2000).
66. B. E. Wendland, E. Aghdassi, C. Tam, J. Carrier, A. H. Steinhart, S. L. Wolman, D. Baron, and J. P. Allard, "Lipid peroxidation and plasma antioxidant micro-nutrients in Crohn's disease," *Am. J. Clin. Nutr.*, **74**, 259 (2001).



67. C. O. Olopade, J. A. Christon, M. Zakkar, C. Hua, W. I. Swedler, P. A. Scheff, and I. Rubinstein, "Exhaled pentane and nitric oxide levels in patients with obstructive sleep apnea." *Chest*, **111**, 1500 (1997).
68. E. Hietanen, H. Bartsch, J. C. Berezat, A. M. Camus, S. McClinton, O. Eremin, L. Davidson, and P. Boyle, "Diet and oxidative stress in breast, colon and prostate cancer patients: A case-control study." *Eur. J. Clin. Nutr.*, **48**, 575 (1994).
69. S. Mendis, P. A. Sobotka, F. L. Leja, and D. E. Euler, "Breath pentane and plasma lipid peroxides in ischemic heart disease." *Free Radic. Biol. Med.*, **19**, 679 (1995).
70. P. J. O'Brien, A. G. Siraki, and N. Shangari, "Aldehyde sources, metabolism, molecular toxicity mechanisms, and possible effects on human health." *Crit. Rev. Toxicol.*, **35**, 609 (2005).
71. S. Ivanova et al., "Neuroprotection incerebral ischemia by neutralization of 3-aminopropanal." *Proc. Natl. Acad. Sci. USA*, **99**, 5579 (2002).
72. W. Li, X. M. Yuan, S. Ivanova, K. J. Tracey, J. W. Eaton, and U. T. Brunk, "3-Aminopropanal, formed during cerebral ischaemia, is a potent lysosomotropic neurotoxin." *Biochem. J.*, **371**, 429 (2003).
73. T. O'Connor, L. S. Ireland, D. J. Harrison, and J. D. Hayes, "Major differences exist in the function and tissue-specific expression of human aflatoxin B1 aldehyde reductase and the principal human aldo-keto reductase AKR1 family members." *Biochem. J.*, **343**, 487 (1999).
74. K. Shinpo, S. Kikuchi, H. Sasaki, A. Ogata, F. Moriawaka, and K. Tashiro, "Selective vulnerability of spinal motor neurons to reactive dicarbonyl compounds, intermediate products of glycation, in vitro: Implication of inefficient glutathione system in spinal motoneurons." *Brain Res.*, **861**, 151 (2000).
75. L. Pavia, G. M. Lampman, G. S. Kriz, and R. G. Engel, in *Introduction to Organic Laboratory Techniques* (Thomson Brooks/Cole) 4th ed., p. 797 (2006).
76. J. M. Sanchez and R. D. Sacks, "GC analysis of human breath with a series-coupled column ensemble and a multibed sorption trap." *Anal. Chem.*, **75**, 2231 (2003).
77. H. Lord, Y. F. Yu, A. Segal, and J. Pawliszyn, "Breath analysis and monitoring by membrane extraction with sorbent interface." *Anal. Chem.*, **74**, 5650 (2002).
78. M. Giardina and S. V. Olesik, "Application of low-temperature glassy carbon-coated macrofibers for solid-phase microextraction analysis of simulated breath volatiles." *Anal. Chem.*, **75**, 1604 (2003).
79. M. Phillips and J. Greenberg, "Method for the collection and analysis of volatile compounds in the breath." *J. Chromatogr. Biomed. Appl.*, **564**, 242 (1991).
80. K. Lamote, P. Brinkman, I. Vandermeersch, M. Vynck, P. J. Sterk, H. Van Langenhove, O. Thas, J. Van Cleemput, K. Nackaerts, and J. P. van Meerbeeck, "Breath analysis by gas chromatography-mass spectrometry and electronic nose to screen for pleural mesothelioma: a cross-sectional case-control study." *Oncotarget*, **8**, 91593 (2017).
81. R. Schnabel, R. Fijten, A. Smolinska, J. Dallinga, M.-L. Boumans, E. Stobberingh, A. Boots, P. Roekaerts, D. Bergmans, and F. Schooten, "Analysis of volatile organic compounds in exhaled breath to diagnose ventilator-associated pneumonia." *Sci. Rep.*, **5**, 1 (2015).
82. M. Beccaria, C. Bobak, B. Maitshotlo, T. R. Mellors, G. Purcaro, F. A. Franchina, C. A. Rees, M. Nasir, A. Black, and J. E. Hill, "Exhaled human breath analysis in active pulmonary tuberculosis diagnostics by comprehensive gas chromatography-mass spectrometry and chemometric techniques." *J. Breath Res.*, **13**, 016005 (2018).
83. C. M. Durán-Acevedo et al., "Exhaled breath analysis for gastric cancer diagnosis in Colombian patients." *Oncotarget*, **9**, 28805 (2018).
84. A. Hansel, A. Jordan, R. Holzinger, P. P. W. Vogel, and W. Lindinger, "Proton transfer reaction mass spectrometry: on-line trace gas analysis at ppb level." *Int. J. Mass Spectrom. Ion Proc.*, **149/150**, 609 (1995).
85. A. Amann, G. Poupart, S. Telser, M. Ledochowski, A. Schmid, and S. Mechtcheriakov, "Applications of breath gas analysis in medicine." *Int. J. Mass Spectrom.*, **239**, 227 (2004).
86. T. Karl, P. Prazeller, D. Mayr, A. Jordan, J. Rieder, R. Fall, and W. Lindinger, "Human breath isoprene and its relation to bloodcholesterol levels: new measurements and modeling." *J. Appl. Physiol.*, **91**, 762 (2001).
87. J. Schmutzhard, J. Rieder, M. Deibl, I. M. Schwentner, S. Schmid, P. Lirk, I. Abraham, and A. R. Gunkel, "Pilot study: volatile organic compounds as a diagnostic marker for head and neck tumors." *Head Neck*, **30**, 743 (2008).
88. A. Boschetti, F. Biasioli, M. van Opbergen, C. Warneke, A. Jordan, R. Holzinger, P. Prazeller, T. Karl, A. Hansel, and W. Lindinger, "PTR-MS real time monitoring of the emission of volatile organic compounds during postharvest aging of berry fruit." *Postharvest Biol. Technol.*, **17**, 143 (1999).
89. N. G. Adams and D. Smith, "The selected ion flow tube (SIFT): A technique for studying ion-neutral reactions." *Int. J. Mass Spectrom. Ion Phys.*, **21**, 349 (1976).
90. P. Spanel, S. Davies, and D. Smith, "Quantification of breath isoprene using the selected ion flow tube mass spectrometric analytical method." *Rapid Commun. Mass Spectrom.*, **13**, 1733 (1999).
91. A. M. Diskin, P. Spanel, and D. Smith, "Time variation of ammonia, acetone, isoprene and ethanol in breath: A quantitative SIFT-MS study over 30 days." *Physiol. Meas.*, **24**, 107 (2003).
92. S. M. Abbott, J. B. Elder, P. Spanel, and D. Smith, "Quantification of acetonitrile in exhaled breath and urinary headspace using selected ion flow tube mass spectrometry." *Int. J. Mass spectrom.*, **228**, 655 (2003).
93. D. Vaira, J. Holton, C. Ricci, C. Basset, L. Gatta, F. Perna, A. Tampieri, and M. Miglioli, "Helicobacter pylori infection from pathogenesis to treatment: a critical reappraisal." *Alimentary Pharmacol. Therapeut.*, **16**(Suppl. 4), 105 (2002).
94. D. Smith and P. Spanel, "The novel selected ion flow tube approach trace gas analysis of air and breath." *Rapid Commun. Mass Spectrom.*, **10**, 1183 (1996).
95. M. A. Samara, W. H. Tang, F. Cikach Jr., Z. Gul, L. Tranchito, K. M. Paschke, J. Vitierna, Y. Wu, D. Laskowski, and R. A. Dweik, "Single exhaled breath metabolomic analysis identifies unique breathprint in patients with acute decompensated heart failure." *J. Am. Coll. Cardiol.*, **61**, 1463 (2013).
96. F. S. Cikach Jr. and R. A. Dweik, "Cardiovascular biomarkers in exhaled breath." *Prog. Cardiovasc. Dis.*, **55**, 34 (2012).
97. N. Alkhouri, F. Cikach, K. Eng, J. Moses, N. Patel, C. Yan, I. Hanouneh, D. Grove, R. Lopez, and R. Dweik, "Analysis of breath volatile organic compounds as a noninvasive tool to diagnose nonalcoholic fatty liver disease in children." *Eur. J. Gastroenterol. Hepatol.*, **26**, 82 (2014).
98. I. A. Hanouneh, N. N. Zein, F. Cikach, L. Dababneh, D. Grove, N. Alkhouri, R. Lopez, and R. A. Dweik, "The breath prints in patients with liver disease identify novel breath biomarkers in alcoholic hepatitis." *Clin. Gastroenterol. Hepatol.*, **12**, 516 (2014).
99. C. Walton, M. Patel, D. Pitts, P. Knight, S. Hoashi, M. Evans, and C. Turner, "The use of a portable breath analysis device in monitoring type 1 diabetes patients in a hypoglycaemic clamp: validation with sift-ms data." *J. Breath Res.*, **8**, 037108 (2014).
100. M. Storer, J. Dummer, H. Lunt, J. Scotter, F. McCartin, J. Cook, M. Swanney, D. Kendall, F. Logan, and M. Epton, "Measurement of breath acetone concentrations by selected ion flow tube mass spectrometry in type 2 diabetes." *J. Breath Res.*, **5**, 046011 (2011).
101. N. Barsan and U. Weimar, "Conduction model of metal oxide gas sensors." *J. Electroceram.*, **7**, 143 (2001).
102. H.-J. Kim and J.-H. Lee, "Highly sensitive and selective gas sensors using p-type oxide semiconductors." *Sensors Actuators B*, **192**, 607 (2014).
103. G. Korotcenkov, V. Brinzari, Y. Boris, M. Ivanov, J. Schwank, and J. Morante, "Influence of surface Pd doping on gas sensing characteristics of SnO<sub>2</sub> thin films deposited by spray pyrolysis." *Thin Solid Films*, **436**, 119 (2003).
104. T. Antonio, R. Marco, and S. E. Pratsinis, "Minimal cross-sensitivity to humidity during ethanol detection by SnO<sub>2</sub>-TiO<sub>2</sub> solid solutions." *Nanotechnology*, **20**, 315502 (2009).
105. T. Antonio, M. Graf, and S. E. Pratsinis, "Optimal doping for enhanced SnO<sub>2</sub> sensitivity and thermal stability." *Adv. Funct. Mater.*, **18**, 1969 (2008).
106. L. Wang, A. Teleki, S. E. Pratsinis, and P. I. Gouma, "Ferroelectric WO<sub>3</sub> nanoparticles for acetone selective detection." *Chem. Mater.*, **20**, 4794 (2008).
107. P. Gouma and K. I. Kalyanasundaram, "A selective nanosensing probe for nitric oxide." *Appl. Phys. Lett.*, **93**, 244102 (2008).
108. M. Righettoni, A. Tricoli, and S. E. Pratsinis, "Thermally stable, silica-doped  $\epsilon$ -WO<sub>3</sub> for sensing of acetone in the human breath." *Chem. Mater.*, **22**, 3152 (2010).
109. M. Righettoni, A. Tricoli, and S. E. Pratsinis, "Si:WO<sub>3</sub> sensors for highly selective detection of acetone for easy diagnosis of diabetes by breath analysis." *Anal. Chem.*, **82**, 3581 (2010).
110. G. Korotcenkov, "Gas response control through structural and chemical modification of metal oxide films: state of the art and approaches." *Sens. Actuators B*, **107**, 209 (2005).
111. A. Tricoli and S. E. Pratsinis, "Dispersed nanoelectrode devices." *Nat. Nanotechnol.*, **5**, 54 (2010).
112. C. S. Rout, M. Hegde, and C. N. R. Rao, "H<sub>2</sub>S sensors based on tungsten oxide nanostructures." *Sens. Actuators B*, **128**, 488 (2008).
113. J. Liu, X. Wang, Q. Peng, and Y. Li, "Vanadium Pentoxide Nanobelts: Highly Selective and Stable Ethanol Sensor Materials." *Adv. Mater.*, **6**, 764 (2005).
114. S. Chakraborty, A. Sen, and H. S. Maiti, "Selective detection of methane and butane by temperature modulation in iron doped tin oxide sensors." *Sens. Actuators B*, **115**, 610 (2006).
115. S.-J. Kim, I.-S. Hwang, C. W. Na, I.-D. Kim, Y. C. Kang, and J.-H. Lee, "Ultrasensitive and selective C<sub>2</sub>H<sub>5</sub>OH sensors using Rh-loaded In<sub>2</sub>O<sub>3</sub> hollow spheres." *J. Mater. Chem.*, **21**, 18560 (2011).
116. J. Tamaki, T. Maekawa, and N. Miura, "CuO-SnO<sub>2</sub> element for highly sensitive and selective detection of H<sub>2</sub>S." *Sens. Actuators B*, **9**, 197 (1992).
117. Y. H. Cho, Y. N. Ko, Y. C. Kang, I.-D. Kim, and J.-H. Lee, "Ultrasensitive and ultrasensitive detection of trimethylamine using MoO<sub>3</sub> nanoplates prepared by ultrasonic spray pyrolysis." *Sens. Actuators B*, **195**, 189 (2014).
118. Y. J. Hong, J.-W. Yoon, J.-H. Lee, and Y. C. Kang, "One-pot synthesis of Pd-loaded SnO<sub>2</sub> yolk-shell nanostructures for ultrasensitive methyl benzene sensors." *Chem. Eur. J.*, **20**, 2737 (2014).
119. S.-Y. Jeong, J.-W. Yoon, T.-H. Kim, H.-M. Jeong, C.-S. Lee, Y. C. Kang, and J.-H. Lee, "Ultra-selective detection of sub-ppm-level benzene using Pd-SnO<sub>2</sub> yolk-shell micro-reactors with a catalytic Co<sub>3</sub>O<sub>4</sub> overlayer for monitoring air quality." *J. Mater. Chem. A*, **5**, 1446 (2017).
120. T. Sahm, W. Rong, N. Barsan, L. Madler, and U. Weimar, "Sensing of CH<sub>4</sub>, CO and ethanol with in situ nanoparticle aerosol-fabricated multilayer sensors." *Sens. Actuators B*, **127**, 63 (2007).
121. H. G. Moon, Y. R. Choi, S. Shim, K.-I. Choi, J.-H. Lee, J.-S. Kim, S.-J. Yoon, H.-H. Park, C.-Y. Kang, and H. W. Jang, "Extremely sensitive and selective NO probe based on villi-like WO<sub>3</sub> nanostructures for application to exhaled breath analyzers." *ACS Appl. Mater. Interfaces*, **5**, 10591 (2013).
122. W.-T. Koo, S.-J. Choi, N.-H. Kim, J.-S. Jang, and I.-D. Kim, "Catalyst-decorated hollow WO<sub>3</sub> nanotubes using layer-by-layer self-assembly on polymeric nanofiber templates and their application in exhaled breath sensor." *Sens. Actuators B*, **223**, 301 (2016).
123. C. Sun, G. Maduraiveeran, and P. Dutta, "Nitric oxide sensors using combination of p- and n-type semiconducting oxides and its application for detecting NO in human breath." *Sens. Actuators B*, **186**, 117 (2013).

124. J. Zhang, S. Wang, Y. Wang, M. Xu, H. Xia, S. Zhang, W. Huang, X. Guo, and S. Wu, "ZnO hollow spheres: preparation, characterization, and gas sensing properties." *Sens. Actuators B*, **139**, 411 (2009).
125. P. Gouma, "Selective Oxide Sensors as Non-Invasive Disease Monitors." *SPIE Newsroom* (2011).
126. B. Frubberger, N. Stirling, F. G. Grillo, S. Ma, D. Ruthven, R. J. Lad, and B. G. Frederick, "Detection and quantification of nitric oxide in human breath using a semiconducting oxide based chemiresistive microsensor." *Sensors Actuators B*, **76**, 226 (2001).
127. D. Mutschall, HolznerK, and E. Obermeier, "Sputtered molybdenum oxide thin films for NH<sub>3</sub> detection." *Sens. Actuators B*, **36**, 320 (1996).
128. C. Imawan, F. Solzbacher, H. Steffes, and E. Obermeier, "Gas-sensing characteristics of modified-MoO<sub>3</sub> thin films using Ti-overlayers for NH<sub>3</sub> gas sensors." *Sens. Actuators B*, **64**, 193 (2000).
129. S. S. Sunu, E. Prabhu, V. Jayaraman, K. I. Gnanasekar, K. SeshagiriT, and T. Gnanasekaran, "Electrical conductivity and gas sensing properties of MoO<sub>3</sub>." *Sens. Actuators B*, **101**, 161 (2004).
130. P. Gouma, K. Kalyanasundaram, X. Yun, M. Stanacevic, and L. Wang, "Nanosensor and breath analyzer for ammonia detection in exhaled human breath." *IEEE Sensors J.*, **10**, 49 (2010).
131. G. Jodhani, J. Huang, and P. Gouma, "Flame spray synthesis and ammonia sensing properties of pure  $\alpha$ -MoO<sub>3</sub> nanosheets." *J. Nanotechnol.*, **2016**, 7016926 (2016).
132. A. K. Prasad, D. J. Kubinski, and P. I. Gouma, "Comparison of sol-gel and ion beam deposited MoO<sub>3</sub> thin film gas sensors for selective ammonia detection." *Sens. Actuators B*, **93**, 25 (2003).
133. D. Kwak, M. Wang, K. J. Koski, L. Zhang, H. Sokol, R. Maric, and Y. Lei, "Molybdenum Trioxide ( $\alpha$ -MoO<sub>3</sub>) Nanoribbons for Ultrasensitive Ammonia (NH<sub>3</sub>) Gas Detection: Integrated Experimental and Density Functional Theory Simulation Studies." *ACS Appl. Mater. Interfaces*, **11**, 10697 (2019).
134. A. T. Günter, M. Righettoni, and S. E. Pratsinis, "Selective sensing of NH<sub>3</sub> by Si-doped  $\alpha$ -MoO<sub>3</sub> for breath analysis." *Sens. Actuators B*, **223**, 266 (2016).
135. V. Srivastava and K. Jain, "Highly sensitive NH<sub>3</sub> sensor using Pt catalyzed silica coating over WO<sub>3</sub> thick films." *Sens. Actuators B*, **133**, 46 (2006).
136. I. Jimenez, M. A. Centeno, R. Scotti, F. Morazzoni, J. Arbiol, A. Cornet, and J. R. Morante, "NH<sub>3</sub> interaction with chromium-doped WO<sub>3</sub> nanocrystalline powders for gas sensing applications." *J. Mater. Chem.*, **14**, 2412 (2004).
137. I. Jimenez, M. A. Centeno, R. Scotti, F. Morazzoni, A. Cornet, and J. R. Morante, "NH<sub>3</sub> interaction with catalytically modified nano-WO<sub>3</sub> powders for gas sensing applications." *J. Electrochem. Soc.*, **150**, H72 (2003).
138. C. Zamani, O. Casals, T. Andreu, J. R. Morante, and A. Romano-Rodriguez, "Detection of amines with chromium-doped WO<sub>3</sub> mesoporous material." *Sens. Actuators B*, **140**, 557 (2009).
139. G. Jeevitha, R. Abhinayaa, D. Mangalaraj, N. Ponpandian, P. Meena, V. Mounasamy, and S. Madanagurusamy, "Porous reduced graphene oxide (rGO)/WO<sub>3</sub> nanocomposites for the enhanced detection of NH<sub>3</sub> at room temperature." *Nanoscale Adv.*, **1**, 1799 (2019).
140. H. Wu, Z. Ma, Z. Lin, H. Song, S. Yan, and Y. Shi, "High-sensitive ammonia sensors based on tin monoxide nanoshells." *Nanomaterials (Basel)*, **9**, E388 (2019).
141. D. Zhang, C. Jiang, and Y. Sun, "Room-temperature high-performance ammonia gas sensor based on layer-by-layer self-assembled molybdenum disulfide/zinc oxide nanocomposite film." *J. Alloys Compd.*, **698**, 476 (2017).
142. M. D'Arienzo, M. Crippa, P. Gentile, C. M. Mari, S. Polizzi, R. Ruffo, R. Scotti, L. Wahba, and F. Morazzoni, "Sol-gel derived mesoporous Pt and Cr-doped WO<sub>3</sub> thin films: the role played by mesoporosity and metal doping in enhancing the gas sensing properties." *J. Sol-Gel Sci. Technol.*, **60**, 378 (2011).
143. D. SenguttuvanT, V. Srivastava, J. S. Tawal, M. Mishraa, S. Srivastava, and K. Jain, "Gas sensing properties of nanocrystalline tungsten oxide synthesized by acid precipitation method." *Sens. Actuators B*, **150**, 384 (2010).
144. Y. Wang et al., "NH<sub>3</sub> gas sensing performance enhanced by Pt-loaded on mesoporous WO<sub>3</sub>." *Sens. Actuators B*, **238**, 473 (2017).
145. N. V. Hieu, V. V. Quang, N. D. Hoa, and D. Kim, "Preparing large-scale WO<sub>3</sub> nanowire-like structure for high sensitivity NH<sub>3</sub> gas sensor through a simple route." *Curr. Appl. Phys.*, **11**, 657 (2011).
146. M. D'Arienzo, L. Armelao, C. M. Mari, S. Polizzi, R. Ruffo, R. Scotti, and F. Morazzoni, "Macroporous WO<sub>3</sub> thin films active in NH<sub>3</sub> sensing: role of the hosted Cr isolated centers and Pt nanoclusters." *J. Am. Chem. Soc.*, **133**, 5296 (2011).
147. L. Wang, J. Pfeifer, C. Balázs, and P. I. Gouma, "Synthesis and sensing properties to NH<sub>3</sub> of hexagonal WO<sub>3</sub> metastable nanopowders." *Mater. Manuf. Process.*, **22**, 773 (2007).
148. Y. M. Zhao and Y. Q. Zhu, "Room temperature ammonia sensing properties of W<sub>18</sub>O<sub>49</sub> nanowires." *Sens. Actuators B*, **137**, 27 (2009).
149. T. A. Ho, T. S. Jun, and Y. S. Kim, "Material and NH<sub>3</sub>-sensing properties of polypyrrole coated tungsten oxide nanofibers." *Sens. Actuators B*, **185**, 523 (2013).
150. G. Wang, Y. Ji, X. Huang, X. Yang, P. I. Gouma, and M. Dudley, "Fabrication and characterization of polycrystalline WO<sub>3</sub> nanofibers and their application for ammonia sensing." *J. Phys. Chem. B*, **110**, 23777-82 (2006).
151. M. Epifani, N. G. Castellote, J. D. Prades, A. Cirera, T. Andreu, J. Arbiol, P. Siciliano, and J. R. Morante, "Suppression of the NO<sub>2</sub> interference by chromium addition in WO<sub>3</sub>-based ammonia sensors. Investigation of the structural properties and of the related sensing pathways." *Sensors Actuators B*, **187**, 308 (2013).
152. D. D. Nguyen, D. V. Dang, and D. C. Nguyen, "Hydrothermal synthesis and NH<sub>3</sub> gas sensing property of WO<sub>3</sub> nanorods at low temperature." *Adv. Nat. Sci.: Nanosci. Nanotechnol.*, **6**, 035006 (2015).
153. R. Ghosh, A. K. Nayak, S. Santra, D. Pradhan, and P. K. Guha, "Enhanced ammonia sensing at room temperature with reduced graphene oxide/ tin oxide hybrid film." *RSC Adv.*, **5**, 50165 (2015).
154. N. V. Toan, C. M. Hung, N. V. Duy, N. D. Hoa, D. T. T. Le, and N. V. Hieu, "Bilayer SnO<sub>2</sub>-WO<sub>3</sub> nanofilms for enhanced NH<sub>3</sub> gas sensing performance." *Mater. Sci. Eng. B*, **224**, 163 (2017).
155. S. Li et al., "The room temperature gas sensor based on Polyaniline@flower-like WO<sub>3</sub> nanocomposites and flexible PET substrate for NH<sub>3</sub> detection." *Sens. Actuators B*, **259**, 505 (2018).
156. N. G. Deshpande, Y. G. Gudage, R. Sharma, J. C. Vyas, J. B. Kim, and Y. P. Lee, "Studies on tin oxide-intercalated polyaniline nanocomposite for ammonia gas sensing applications." *Sens. Actuators B*, **138**, 76 (2009).
157. X. Wang, D. Gu, X. Li, S. Lin, S. Zhao, M. N. Romyantseva, and A. M. Gaskov, "Reduced graphene oxide hybridized with WS<sub>2</sub> nanoflakes based heterojunctions for selective ammonia sensors at room temperature." *Sens. Actuators B*, **282**, 290 (2019).
158. E. Singh, M. Meyyappan, and H. S. Nalwa, "Flexible graphene-based wearable gas and chemical sensors." *ACS Appl. Mater. Interfaces*, **9**, 34544 (2017).
159. J. M. Tulliani, A. Cavaliere, S. Musso, E. Sardella, and F. Geobaldo, "Room temperature ammonia sensors based on zinc oxide and functionalized graphite and multi-walled carbon nanotubes." *Sens. Actuators B*, **152**, 144 (2011).
160. S.-J. Choi, I. Lee, B.-H. Jang, D.-Y. Youn, W.-H. Ryu, C. O. Park, and I.-D. Kim, "Selective diagnosis of diabetes using Pt-functionalized WO<sub>3</sub> hemitube networks as a sensing layer of acetone in exhaled breath." *Anal. Chem.*, **85**, 1792 (2013).
161. S.-J. Choi, S.-J. Kim, H.-J. Cho, J.-S. Jang, Y.-M. Lin, H. L. Tuller, G. C. Rutledge, and I.-D. Kim, "WO<sub>3</sub> nanofiber-based biomarker detectors enabled by protein-encapsulated catalyst self-assembled on polystyrene colloid templates." *Small*, **12**, 911 (2016).
162. S.-J. Kim, S.-J. Choi, J.-S. Jang, N.-H. Kim, M. Hakim, H. L. Tuller, and I.-D. Kim, "Mesoporous WO<sub>3</sub> nanofibers with protein-templated nanoscale catalysts for detection of trace biomarkers in exhaled breath." *ACS Nano*, **10**, 5891 (2016).
163. M. Righettoni, A. Tricoli, S. Gass, A. Schmid, A. Amann, and S. E. Pratsinis, "Breath acetone monitoring by portable Si:WO<sub>3</sub> gas sensors." *Anal. Chim. Acta*, **738**, 69 (2012).
164. K. H. Kim, S.-J. Kim, H.-J. Cho, N.-H. Kim, J.-S. Jang, S.-J. Choi, and I.-D. Kim, "WO<sub>3</sub> nanofibers functionalized by protein-templated RuO<sub>2</sub> nanoparticles as highly sensitive exhaled breath gas sensing layers." *Sens. Actuators B*, **241**, 1276 (2017).
165. N.-H. Kim, S.-J. Choi, S.-J. Kim, H.-J. Cho, J.-S. Jang, W.-T. Koo, M. Kim, and I.-D. Kim, "Highly sensitive and selective acetone sensing performance of WO<sub>3</sub> nanofibers functionalized by Rh<sub>2</sub>O<sub>3</sub> nanoparticles." *Sens Actuators B*, **224**, 185 (2016).
166. H. Xu et al., "Mesoporous WO<sub>3</sub> nanofibers with crystalline framework for high-performance acetone sensing." *Front. Chem.*, **7**, 266 (2019).
167. A. Sen and S. Rana, A sensor composition for acetone detection in breath, PCT no. WO2013164836A1 (2013).
168. C. Yali, Y. Wang, J. Zhang, H. Li, L. Liu, Y. Li, L. Du, and H. Duan, "A comparison of Eu-doped  $\alpha$ -Fe<sub>2</sub>O<sub>3</sub> nanotubes and nanowires for acetone sensing." *Nano Brief Rep. Rev.*, **12**, 1750138 (2017).
169. M. Narjinary, P. Rana, and M. Pal, "Enhanced and selective acetone sensing properties of SnO<sub>2</sub>-MWCNT nanocomposites: Promising materials for diabetes sensor." *Mater. Des.*, **115**, 158 (2017).
170. S. Chakraborty and M. Pal, "Highly selective and stable acetone sensor based on chemically prepared bismuth ferrite nanoparticles." *J. Alloys Compd.*, **787**, 1204 (2019).
171. A. A. Abokifa, K. Haddad, J. Fortner, C. S. Lo, and P. Biswas, "Sensing mechanism of ethanol and acetone at room temperature by SnO<sub>2</sub> nano-columns synthesized by aerosol routes: theoretical calculations compared to experimental results." *J. Mater. Chem. A*, **6**, 2053 (2018).
172. M. J. Priya, P. M. Aswathy, M. K. Kavitha, M. K. Jayaraj, and K. R. Kumar, "Improved acetone sensing properties of electrospun Au-doped SnO<sub>2</sub> nanofibers." *AIP Conf. Proc.*, **2082**, 030026 (2019).
173. M. S. Preethi, S. P. Bharath, and K. V. Bangera, "Spray deposited gallium doped tin oxide thinfilm for acetone sensor application." *AIP Conf. Proc.*, **1943**, 020088 (2018).
174. Z. E. Khalidi, B. Hartiti, M. Siadat, E. Comini, H. M. M. M. Arachchige, S. Fadili, and P. Thevenin, "Acetone sensor based on Ni doped ZnO nanostructures: growth and sensing capability." *J. Mater. Sci., Mater. Electron.*, **30**, 7681 (2019).
175. X. Xing, N. Chen, Y. Yang, R. Zhao, Z. Wang, Z. Wang, T. Zou, and Y. Wang, "Pt-functionalized nanoporous TiO<sub>2</sub> nanoparticles with enhanced gas sensing performances toward acetone." *Phys. Status Solidi A*, **215**, 1800100 (2018).
176. W. Liu, L. Xu, K. Sheng, X. Zhou, B. Dong, G. Lu, and H. Song, "A highly sensitive and moisture-resistant gas sensor for diabetes diagnosis with Pt@In<sub>2</sub>O<sub>3</sub> nanowires and a molecular sieve for protection." *NPG Asia Materials*, **10**, 293 (2018).
177. KJ-W Yoon, J-S Kim, T-H Kim, Y J. Jong, Y C Kang, and J-H Lee, "A new strategy for humidity independent oxide chemiresistors: dynamic self-refreshing of In<sub>2</sub>O<sub>3</sub> sensing surface assisted by layer-by-layer coated CeO<sub>2</sub> nanoclusters." *Small*, **12**, 4229 (2016).
178. J.-S. Jang, S.-J. Chio, S.-J. Kim, M. Hakim, and I.-D. Kim, "Rational design of highly porous SnO<sub>2</sub> nanotubes functionalized with biomimetic nanocatalysts for direct observation of simulated diabetes." *Adv. Funct. Mater.*, **26**, 4740 (2016).
179. J. Shin, S.-J. Chio, I. Lee, D.-Y. Youn, C. O. Park, J.-H. Lee, H. L. Tuller, and I.-D. Kim, "Thin-wall assembled SnO<sub>2</sub> fibers functionalized by catalytic Pt nanoparticles and their superior exhaled-breath-sensing properties for the diagnosis of diabetes." *Adv. Funct. Mater.*, **23**, 2357 (2013).
180. W.-T. Koo, S.-J. Chio, J.-S. Jang, and I.-D. Kim, "Metal-organic framework templated synthesis of ultrasmall catalyst loaded ZnO/ZnCo<sub>2</sub>O<sub>4</sub> hollow spheres for enhanced gas sensing properties." *Sci. Rep.*, **7**, 45074 (2017).

181. L. Cheng, S. Y. Ma, X. B. Li, J. Luo, W. Q. Li, F. M. Li, Y. Z. Mao, T. T. Wang, and Y. F. Li, "Highly sensitive acetone sensors based on Y-doped SnO<sub>2</sub> prismatic hollow nanofibers synthesized by electrospinning." *Sens. Actuators B*, **200**, 181 (2014).
182. W. Chen, Z. Qin, Y. Liu, Y. Zhang, Y. Li, S. Shen, Z. M. Wang, and H.-Z. Song, "Promotion on acetone sensing of single SnO<sub>2</sub> nanobelt by Eu doping." *Nanoscale Res. Lett.*, **12**, 405 (2017).
183. T. Godish, in *Indoor Air Pollution Control*. (Lewis Publishers, Pearl River, NY) (1991).
184. A. I. Ayeshe, S. T. Mahmoud, S. J. Ahmad, and Y. Haik, "Novel hydrogen gas sensor based on Pd and SnO<sub>2</sub> nanoclusters." *Mater. Lett.*, **128**, 354 (2014).
185. L. P. Chikhale, J. Y. Patil, A. V. Rajgure, F. I. Shaikh, I. S. Mulla, and S. S. Suryavanshi, "Cocprecipitation synthesis of nanocrystalline SnO<sub>2</sub>: effect of Fe doping on structural, morphological, optical and ethanol vapor response properties." *Measurement*, **57**, 46 (2014).
186. J. Q. Xu, X. H. Jia, X. D. Lou, G. X. Xi, J. J. Han, and Q. H. Gao, "Selective detection of HCHO gas using mixed oxides of ZnO/ZnSnO<sub>3</sub>." *Sens. Actuators B*, **120**, 694 (2007).
187. F. Li, T. Zhang, X. Gao, R. Wang, and B. Li, "Coaxial electrospinning heterojunction SnO<sub>2</sub>/Au-doped In<sub>2</sub>O<sub>3</sub> core-shell nanofibers for acetone gas sensor." *Sens. Actuators B*, **252**, 822 (2017).
188. P. Sun, Y. Cai, S. Du, X. Xu, L. You, J. Ma, F. Liu, X. Liang, Y. Sun, and G. Lu, "Hierarchical  $\alpha$ -Fe<sub>2</sub>O<sub>3</sub>/SnO<sub>2</sub> semiconductor composites: hydrothermal synthesis and gas sensing properties." *Sens. Actuators B*, **182**, 336 (2013).
189. L. Cheng, S. Y. Ma, T. T. Wang, and J. Luo, "Synthesis and enhanced acetone sensing properties of 3D porous flower-like SnO<sub>2</sub> nanostructures." *Mater. Lett.*, **143**, 84 (2015).
190. V. V. Krivitsky, D. V. Petukhov, A. A. Eliseev, A. V. Smirnov, M. N. Rumyantseva, and A. M. Gaskov, "Acetone sensing by modified SnO<sub>2</sub> nanocrystalline sensor materials." *Nanotechnol. Basis Adv. Sens.*, 409 (2011).
191. K. Suematsu, N. Ma, K. Watanabe, M. Yuasa, T. Kida, and K. Shimanoe, "Effect of humid aging on the oxygen adsorption in SnO<sub>2</sub> gas sensors." *Sensors*, **18**, 254 (2018).
192. N. Makisimovich, V. Vorotnytsyev, N. Nikitina, O. Kaskevich, P. Karabum, and F. Martynenko, "Adsorption semiconductor sensor for diabetic ketoacidosis diagnosis." *Sens. Actuators B*, **36**, 419 (1996).
193. S. Zhu, D. Zhang, J. Gu, J. Xu, J. Dong, and J. Li, "Biotemplate fabrication of SnO<sub>2</sub> nanotubular materials by a sonochemical method for gas sensors." *J. Nanopart. Res.*, **12**, 1389 (2010).
194. H. Yu, S. Wang, C. Xiao, B. Xiao, P. Wang, Z. Li, and M. Zhang, "Enhanced acetone gas sensing properties by aurelia-like SnO<sub>2</sub> micronanostructures." *Cryst. Eng. Comm.*, **17**, 4316 (2015).
195. N. Bärtsch and U. Weimar, "Understanding the fundamental principles of metal oxide based gas sensors: the example of CO sensing with SnO<sub>2</sub> sensors in the presence of humidity." *J. Phys. Condens. Matter*, **15**, R813 (2003).
196. M. R. Yang, S. Y. Chu, and R. C. Chang, "Synthesis and study of the SnO<sub>2</sub> nanowires growth." *Sens. Actuators B*, **122**, 269 (2007).
197. H. Zhang, H. Qin, C. Gao, and J. Hu, "An Ultrahigh Sensitivity Acetone Sensor Enhanced by Light Illumination." *Sensors (Basel)*, **18**, 2318 (2018).
198. Z. Jiang, M. Yin, and C. Wang, "Facile synthesis of Ca<sup>2+</sup>/Au co-doped SnO<sub>2</sub> nanofibers and their application in acetone sensor." *Mater. Lett.*, **194**, 209 (2017).
199. N. E. Wongrat, C. Chanlek, and Ch W. Thup, "Acetone gas sensors based on ZnO nanostructures decorated with Pt and Nb." *Ceram. Inter.*, **43**, S557 (2017).
200. Z. El khaldi, E. Comini, B. Hartiti, and A. Mounen, "Effect of vanadium doping on ZnO sensing properties synthesized by spray pyrolysis." *Mater. Des.*, **139**, 56 (2018).
201. S. Steinhauer, E. Brunet, T. Maier, G. C. Mutinati, KöckA, O. Freudenberg, C. Gspan, W. Grogger, A. Neuhold, and R. Resel, "Gas sensing properties of novel CuO nanowire devices." *Sens. Actuators B*, **187**, 50 (2013).
202. J. Chen, K. Wang, L. Hartman, and W. Zhou, "H<sub>2</sub>S detection by vertically aligned CuO nanowire array sensors." *J. Phys. Chem. C*, **112**, 16017 (2008).
203. F. Zhang, A. Zhu, Y. Luo, Y. Tian, J. Yang, and Y. Qin, "CuO nanosheets for sensitive and selective determination of H<sub>2</sub>S with high recovery ability." *J. Phys. Chem. C*, **114**, 19214 (2010).
204. N. S. Ramgir, S. K. Ganapathi, M. Kaur, N. Datta, K. P. Muthe, D. K. Aswal, S. K. Gupta, and J. V. Yakhmi, "Sub-ppm H<sub>2</sub>S sensing at room temperature using CuO thin films." *Sens. Actuators B*, **151**, 90 (2010).
205. Y. Qin, F. Zhang, Y. Chen, Y. Zhou, J. Li, A. Zhu, Y. Luo, Y. Tian, and J. Yang, "Hierarchically porous CuO hollow spheres fabricated via a one-pot template-free method for high-performance gas sensors." *J. Phys. Chem. C*, **116**, 11994 (2012).
206. J. Tamaki, K. Shimanoe, Y. Yamada, Y. Yamamoto, N. Miura, and N. Yamazoe, "Dilute hydrogen sulfide sensing properties of CuO-SnO<sub>2</sub> thin film prepared by low-pressure evaporation method." *Sens. Actuators B*, **49**, 121 (1998).
207. I. Giebelhaus, E. Varchukina, T. Fischer, M. Rumyantseva, V. Ivanov, A. Gaskov, J. R. Morante, J. Arbiol, W. Tyrre, and S. Mathur, "One-Dimensional CuO-SnO<sub>2</sub> p-n Heterojunctions for Enhanced Detection of H<sub>2</sub>S." *J. Mater. Chem. A*, **1**, 11261 (2013).
208. X. Xue, L. Xing, Y. Chen, S. Shi, Y. Wang, and T. Wang, "Synthesis and H<sub>2</sub>S sensing properties of CuO-SnO<sub>2</sub> core/shell PN-junction nanorods." *J. Phys. Chem. C*, **112**, 12157 (2008).
209. I.-S. Hwang, J.-K. Choi, S.-J. Kim, K.-Y. Dong, J.-H. Kwon, B.-K. Ju, and J.-H. Lee, "Enhanced H<sub>2</sub>S sensing characteristics of SnO<sub>2</sub> nanowires functionalized with CuO." *Sens. Actuators B*, **142**, 105 (2009).
210. K.-I. Choi, H.-J. Kim, Y. C. Kang, and J.-H. Lee, "Ultrasensitive and ultrasensitive detection of H<sub>2</sub>S in highly humid atmosphere using CuO-loaded SnO<sub>2</sub> hollow spheres for real-time diagnosis of halitosis." *Sens. Actuators B*, **194**, 371 (2014).
211. J. Ma, Y. Liu, H. Zhang, P. Ai, N. Gong, Y. Wu, and D. Yu, "Room temperature ppb level H<sub>2</sub>S detection of a single Sb-doped SnO<sub>2</sub> nanoribbon device." *Sens. Actuators B*, **216**, 72 (2015).
212. X. Liang, T.-H. Kim, J.-W. Yoon, C.-H. Kwak, and J.-H. Lee, "Ultrasensitive and ultrasensitive detection of H<sub>2</sub>S using electrospun CuO-loaded In<sub>2</sub>O<sub>3</sub> nanofiber sensors assisted by pulse heating." *Sens. Actuators B*, **209**, 934 (2015).
213. S.-J. Kim, C. W. Na, I.-S. Hwang, and J.-H. Lee, "One-pot hydrothermal synthesis of CuO-ZnO composite hollow spheres for selective H<sub>2</sub>S detection." *Sens. Actuators B*, **168**, 83 (2012).
214. K. C.-H. WooH-S, I.-D. Kim, and J.-H. Lee, "Selective, sensitive, and reversible H<sub>2</sub>S sensors using Mo-doped ZnO nanowire networks." *J. Mater. Chem. A*, **2**, 6412 (2014).
215. H.-L. Yu, L. Li, X.-M. Gao, Y. Zhang, F. Meng, T.-S. Wang, G. Xiao, Y.-J. Chen, and C.-L. Zhu, "Synthesis and H<sub>2</sub>S gas sensing properties of cage-like  $\alpha$ -MoO<sub>3</sub>/ZnO composite." *Sens. Actuators B*, **171-172**, 679 (2012).
216. V. Galstyan, N. Poli, and E. Comini, "Highly sensitive and selective H<sub>2</sub>S chemical sensor based on ZnO nanomaterial." *Appl. Sci.*, **9**, 1167 (2019).
217. C. Wang, X. Chu, and M. Wu, "Detection of H<sub>2</sub>S down to ppb levels at room temperature using sensors based on ZnO nanorods." *Sens. Actuators B*, **113**, 320 (2006).
218. H.-Y. Li, L. Huang, X.-X. Wang, C.-S. Lee, J.-W. Yoon, J. Zhou, X. Guo, and J.-H. Lee, "Molybdenum trioxide nanopaper as a dual gas sensor for detecting trimethylamine and hydrogen sulfide." *RSC Adv.*, **7**, 3680 (2017).
219. X. Gao, C. Li, Z. Yin, and Y. Chen, "Synthesis and H<sub>2</sub>S sensing performance of MoO<sub>3</sub>/Fe<sub>2</sub>(MoO<sub>4</sub>)<sub>3</sub> yolk/shell nanostructures." *RSC Adv.*, **5**, 37703 (2015).
220. S. Kabcum, N. Tammanoon, A. Wisitsaraat, A. Tuantranont, S. Phanichphant, and C. Liewhiran, "Role of molybdenum substitutional dopants on H<sub>2</sub>S-sensing enhancement of flame-spray-made SnO<sub>2</sub> nanoparticulate thick films." *Sensors Actuators B*, **235**, 678 (2016).
221. J.-W. Yoon, Y. J. Hong, Y. C. Kang, and J.-H. Lee, "High performance chemiresistive H<sub>2</sub>S sensors using Ag-loaded SnO<sub>2</sub> yolk-shell nanostructures." *RSC Adv.*, **4**, 16067 (2014).
222. S. Ma, J. Jia, Y. Tian, L. Cao, S. Shi, X. Li, and X. Wang, "Improved H<sub>2</sub>S sensing properties of Ag/TiO<sub>2</sub> nanofibers." *Ceram. Int.*, **42**, 2041 (2016).
223. Y. Wang, Y. Wang, J. Cao, F. Kong, H. Xia, J. Zhang, B. Zhu, S. Wang, and S. Wu, "Low-temperature H<sub>2</sub>S sensors based on Ag-doped  $\alpha$ -Fe<sub>2</sub>O<sub>3</sub> nanoparticles." *Sens. Actuators B*, **131**, 183 (2008).
224. K. Tian, X.-X. Wang, Z.-Y. Yu, H.-Y. Li, and X. Guo, "Hierarchical and hollow Fe<sub>2</sub>O<sub>3</sub> nanoboxes derived from metal-organic frameworks with excellent sensitivity to H<sub>2</sub>S." *ACS Appl. Mater. Interfaces*, **9**, 29669 (2017).
225. J. Ma, L. Mei, Y. Chen, Q. Li, T. Wang, Z. Xu, X. Duan, and W. Zheng, " $\alpha$ -Fe<sub>2</sub>O<sub>3</sub> nanochains: ammonium acetate-based ionothermal synthesis and ultrasensitive sensors for low-ppm-level H<sub>2</sub>S gas." *Nanoscale*, **5**, 895 (2013).
226. V. Balouria, N. S. Ramgir, A. Singh, A. K. Debnath, A. Mahajan, R. K. Bedi, D. K. Aswal, and S. K. Gupta, "Enhanced H<sub>2</sub>S sensing characteristics of Au modified Fe<sub>2</sub>O<sub>3</sub> thin films." *Sens. Actuators B*, **219**, 125 (2015).
227. R. Lonescu, A. Hoel, C. G. Granqvist, E. Llobet, and P. Heszler, "Low-level detection of ethanol and H<sub>2</sub>S with temperature-modulated WO<sub>3</sub> nanoparticle gas sensors." *Sens. Actuators B*, **104**, 132 (2005).
228. N. H. Kim, S.-J. Choi, D.-J. Yang, J. Bae, J. Park, and I.-D. Kim, "Highly sensitive and selective hydrogen sulfide and toluene sensors using Pd functionalized WO<sub>3</sub> nanofibers for potential diagnosis of halitosis and lung cancer." *Sens. Actuators B*, **193**, 574 (2014).
229. N. Datta, N. Ramgir, M. Kaur, M. Roy, R. Bhatt, S. Kailasaganapathi, A. K. Debnath, D. K. Aswal, and S. K. Gupta, "Vacuum deposited WO<sub>3</sub> thin films based sub-ppm H<sub>2</sub>S sensor." *Mater. Chem. Phys.*, **134**, 851 (2012).
230. S. T. Navale, C. Liu, P. S. Gaikar, V. B. Patil, R. U. R. Sagar, B. Du, R. S. Manee, and F. J. Stadler, "Solution-processed rapid synthesis strategy of Co<sub>3</sub>O<sub>4</sub> for the sensitive and selective detection of H<sub>2</sub>S." *Sens. Actuators B*, **245**, 524 (2017).
231. R. P. Patil, P. V. More, G. H. Jain, P. K. Khanna, and V. B. Gaikwad, "BaTiO<sub>3</sub> nanostructures for H<sub>2</sub>S gas sensor: influence of band-gap, size and shape on sensing mechanism." *Vacuum*, **146**, 445 (2018).
232. C. Balamurugan and D. W. Lee, "Perovskite hexagonal YMnO<sub>3</sub> nanopowder as p-type semiconductor gas sensor for H<sub>2</sub>S detection." *Sens. Actuators B*, **221**, 857 (2015).
233. G. N. Chaudhari, M. Alvi, H. G. Wankhade, A. B. Bodade, and S. V. Manorama, "Nanocrystalline chemically modified CdIn<sub>2</sub>O<sub>4</sub> thick films for H<sub>2</sub>S gas sensor." *Thin Solid Films*, **520**, 4057 (2012).
234. S. V. Jagtap, A. V. Kadu, V. S. Sangawar, S. V. Manorama, and G. N. Chaudhari, "H<sub>2</sub>S sensing characteristics of La<sub>0.7</sub>Pb<sub>0.3</sub>Fe<sub>0.4</sub>Ni<sub>0.6</sub>O<sub>3</sub> based nanocrystalline thick film gas sensor." *Sens. Actuators B*, **131**, 290 (2008).
235. C. Xu, J. Tamaki, N. Miura, and N. Yamazoe, "Grain size effects on gas sensitivity of porous SnO<sub>2</sub>-based elements." *Sens. Actuators B*, **3**, 147 (1991).
236. A. Tricoli, M. Righettoni, and S. E. Pratsinis, "Minimal cross-sensitivity to humidity during ethanol detection by SnO<sub>2</sub>-TiO<sub>2</sub> solid solution." *Nanotechnology*, **20**, 315502 (2009).
237. D. J. Late et al., "Sensing behavior of atomically thin-layered MoS<sub>2</sub> transistors." *ACS Nano*, **7**, 4879 (2013).
238. Q. He, Z. Zeng, Z. Yin, H. Li, S. Wu, X. Huang, and H. Zhang, "Fabrication of flexible MoS<sub>2</sub> thin-film transistor arrays for practical gas-sensing applications." *Small*, **8**, 2994 (2012).



239. N. Yu, L. Wang, M. Li, X. Sun, T. Hou, and Y. Li, "Molybdenum disulfide as a highly efficient adsorbent for non-polar gases." *Phys. Chem. Chem. Phys.*, **17**, 11700 (2015).
240. D. R. Kauffman and A. Star, "Carbon nanotube gas and vapor sensors." *Angew. Chem. Int. Ed.*, **47**, 6550 (2008).
241. T. Zhang, S. Mubeen, N. V. Myung, and M. A. Deshusses, "Recent progress in carbon nanotube-based gas sensors." *Nanotechnology*, **19**, 332001 (2008).
242. O. K. Varghese, P. D. Kichambre, D. Gong, K. G. Ong, E. C. Dickey, and C. A. Grimes, "Gas sensing characteristics of multi-wall carbon nanotubes." *Sens. Actuators B*, **81**, 32 (2001).
243. J. A. Robinson, E. S. Snow, S. C. Badescu, T. L. Reinecke, and F. K. Perkins, "Role of defects in single-walled carbon nanotube chemical sensors." *Nano Lett.*, **6**, 1747 (2006).
244. M. F. L. De Volder, S. H. Tawfik, R. H. Baughman, and A. J. Hart, "Carbon nanotubes: present and future commercial applications." *Science*, **339**, 535 (2013).
245. Y. Dan, Y. Lu, N. J. Kybert, Z. Luo, and A. T. C. Johnson, "Intrinsic response of graphene vapor sensors." *Nano Lett.*, **9**, 1472 (2009).
246. O. Leenaerts, B. Partoens, and F. M. Peeters, "Adsorption of H<sub>2</sub>O, NH<sub>3</sub>, CO, NO<sub>2</sub>, and NO on graphene: a first-principles study." *Phys. Rev. B*, **77**, 125416 (2008).
247. C. R. Minitha, V. S. Anitha, V. Subramaniam, and R. T. S. Kumar, "Impact of oxygen functional groups on reduced graphene oxide based sensors for ammonia and toluene detection at room temperature." *ACS Omega*, **3**, 4105 (2018).
248. J. T. Robinson, F. K. Perkins, E. S. Snow, Z. Wei, and P. E. Sheehan, "Reduced graphene oxide molecular sensors." *Nano Lett.*, **8**, 3137 (2008).
249. J. Suehiro, G. Zhou, H. Imakire, W. Ding, and M. Hara, "Controlled fabrication of carbon nanotube NO<sub>2</sub> gas sensor using dielectrophoretic impedance measurement." *Sens. Actuators B*, **108**, 398 (2005).
250. J. D. Fowler, M. J. Allen, V. C. Tung, Y. Yang, R. B. Kaner, and B. H. Weiller, "Practical chemical sensors from chemically derived graphene." *ACS Nano*, **3**, 301 (2009).
251. A. Karthigeyan, N. Minami, and K. Iakoubovskii, "Highly sensitive, room-temperature gas sensors prepared from cellulose derivative assisted dispersions of single-wall carbon nanotubes." *Jpn. J. Appl. Phys.*, **47**, 7440 (2008).
252. A. Singh, M. A. Uddin, T. Sudarshan, and G. Koley, "Tunable reverse-biased graphene/silicon heterojunction schottky diode sensor." *Small*, **8**, 1555 (2014).
253. L. T. Duy, D.-J. Kim, T. Q. Trung, V. Q. Dang, B.-Y. Kim, H. K. Moon, and N.-E. Lee, "High performance three-dimensional chemical sensor platform using reduced graphene oxide formed on high aspect-ratio micro-pillars." *Adv. Funct. Mater.*, **25**, 883 (2015).
254. S. R. Ng, C. X. Guo, and C. M. Li, "Highly sensitive nitric oxide sensing using three-dimensional graphene/ionic liquid nanocomposite." *Electroanalysis*, **23**, 442 (2011).
255. I.-D. Kim, S.-J. Choi, S.-J. Kim, and J.-S. Jang, in *Exhaled Breath Sensors; In Smart Sensors for Health and Environment Monitoring* (Springer, Dordrecht, New York) p. 19 (2015).
256. R. Baron and J. Saffell, "Amperometric gas sensors as a low cost emerging technology platform for air quality monitoring applications: a review." *ACS Sens.*, **2**, 1553 (2017).
257. R. D. Stewart, R. S. Stewart, W. Stamm, and R. P. Seelen, "Rapid estimation of carboxyhemoglobin level in fire fighters." *JAMA*, **235**, 390 (1976).
258. H. J. Vreman, D. K. Stevenson, W. Oh, A. A. Fanaroff, L. L. Wright, J. A. Lemons, E. Wright, S. Shankaran, J. E. Tyson, and S. B. Korones, "Semiportable electrochemical instrument for determining carbon monoxide in breath." *Clin. Chem.*, **40**, 1927 (1994).
259. T. Hemmingsson, D. Linnarsson, and R. Gamber, "Novel hand-held device for exhaled nitric oxide-analysis in research and clinical applications." *J. Clin. Monit. Comput.*, **18**, 379 (2004).
260. S. P. Mondal, P. K. Dutta, G. W. Hunter, B. J. Ward, D. Laskowski, and R. A. Dweik, "Development of high sensitivity potentiometric NOx sensor and its application to breath analysis." *Sens. Actuators B*, **158**, 292 (2011).
261. J. Obermeier, P. Trefz, K. Wex, B. Sabel, J. K. Schubert, and W. Miekisch, "Electrochemical sensor system for breath analysis of aldehydes, CO and NO." *J. Breath Res.*, **9**, 016008 (2015).
262. J. Wiedemair, H. D. van Dorp, W. Olthuis, and A. van den Berg, "Developing an amperometric hydrogen peroxide sensor for an exhaled breath analysis system." *Electrophoresis*, **33**, 3181 (2012).
263. Y. Zhang, G. Gao, Q. Qian, and D. Cui, "Chloroplasts-mediated biosynthesis of nanoscale Au-Ag alloy for 2-butanone assay based on electrochemical sensor." *Nanoscale Res. Lett.*, **7**, 475 (2012).
264. A. Gholizadeh, D. Voiry, C. Weisel, A. Gow, R. Laumbach, H. Kipen, M. Chhowalla, and M. Javanmard, "Toward point-of-care management of chronic respiratory conditions: Electrochemical sensing of nitrite content in exhaled breath condensate using reduced graphene oxide." *Microsyst. Nanoeng.*, **3**, 17022 (2017).
265. K. Mitsubayashi, H. Matsunaga, G. Nishio, S. Toda, and Y. Nakanishi, "Bioelectronic sniffers for ethanol and acetaldehyde in breath air after drinking." *Biosens. Bioelectron.*, **20**, 1573 (2005).
266. S. Kawahara, Y. Fuchigami, S. Shimokawa, Y. Nakamura, T. Kuretake, M. Kamahori, and S. Uno, "Portable electrochemical gas sensing system with a paper-based enzyme electrode." *Telkomnika*, **15**, 895 (2017).
267. Y. R. Smith, D. Bhattacharya, S. K. Mohanty, and M. Misra, "Anodic functionalization of titania nanotube arrays for the electrochemical detection of tuberculosis biomarker vapors." *J. Electrochem. Soc.*, **163**, B83 (2016).
268. D. Bhattacharya, Y. R. Smith, S. K. Mohanty, and M. Misra, "Titania nanotube array sensor for electrochemical detection of four predominate tuberculosis volatile biomarkers." *J. Electrochem. Soc.*, **163**, B206 (2016).
269. E. Aparicio-Martínez, V. Osuna, R. B. Domínguez, A. Márquez-Lucero, E. A. Zaragoza-Contreras, and A. Vega-Rios, "Room temperature detection of acetone by a PANI/Cellulose/WO<sub>3</sub> electrochemical sensor." *J. Nanomater.*, **2018**, 6519694 (2018).
270. J. Sorocki and A. Rydosz, "A prototype of a portable gas analyzer for exhaled acetone detection." *Appl. Sci.*, **9**, 1 (2019).
271. T. Madasamy, M. Pandiaraj, M. Balamurugan, S. Karnewar, A. R. Benjamin, K. A. Venkatesh, K. Vairamani, S. Kotamraju, and C. Karunakaran, "Virtual electrochemical nitric oxide analyzer using copper, zinc superoxide dismutase immobilized on carbon nanotubes in polypyrrole matrix." *Talanta*, **100**, 168 (2012).
272. O. Kuzmich, B. L. Allen, and A. Star, "Carbon nanotube sensors for exhaled breath components." *Nanotechnology*, **18**, 375502 (2007).
273. K. W. Kao, M. C. Hsu, Y. H. Chang, S. Gwo, and J. A. Yeh, "A sub-ppm acetone gas sensor for diabetes detection using 10 nm thick ultrathin InN FETs." *Sensors*, **12**, 7157 (2012).
274. B. P. de Lacy Costello, R. J. Ewen, N. M. Ratcliffe, and M. Richards, "The characteristics of novel low-cost sensors for volatile biomarker detection." *J. Breath Res.*, **2**, 037017 (2008).
275. F. Gu, X. Yin, H. Yu, P. Wang, and L. Tong, "Polyaniline/polystyrene single-nanowire devices for highly selective optical detection of gas mixtures." *Opt. Express*, **17**, 11230 (2009).
276. NA Yebo, SP Sree, E Levrau, D Christophe, Z Hens, A Martens, and R Baets, "Selective and reversible ammonia gas detection with nanoporous film functionalized silicon photonic micro-ring resonator." *Optics Express*, **20**, 11855 (2012).
277. G. Peng, E. Trock, and H. Haick, "Detecting simulated patterns of lung cancer biomarkers by random network of single-walled carbon nanotubes coated with non-polymeric organic materials." *Nano Lett.*, **8**, 3631 (2008).
278. N. Peled, M. Hakim, P. A. Bunn Jr, Y. E. Miller, T. C. Kennedy, J. Mattei, J. D. Mitchell, F. R. Hirsch, and H. Haick, "Non-invasive breath analysis of pulmonary nodules." *J. Thorac. Oncol.*, **7**, 1528 (2012).
279. G. Peng, M. Hakim, Y. Y. Broza, S. Billan, R. Abdah-Bortnyak, A. Kuten, U. Tisch, and H. Haick, "Detection of lung, breast, colorectal, and prostate cancers from exhaled breath using a single array of nanosensors." *Br. J. Cancer*, **103**, 542 (2010).
280. M. Hakim, S. Billan, U. Tisch, G. Peng, I. Dvorkind, O. Marom, R. Abdah-Bortnyak, A. Kuten, and H. Haick, "Diagnosis of head and neck cancer from exhaled breath." *Br. J. Cancer*, **104**, 1649 (2011).
281. Y. Y. Broza, R. Kremer, U. Tisch, A. Gevorkyan, A. Shiban, L. A. Best, and H. Haick, "A nanomaterial-based breath test for short-term follow-up after lung tumor resection." *Nanomedicine*, **9**, 15 (2012).
282. E. A. Chapman, P. S. Thomas, E. Stone, C. Lewis, and D. H. Yates, "A breath test for malignant mesothelioma using an electronic nose." *Eur. Respir. J.*, **40**, 448 (2012).
283. S. Dragonieri et al., "An electronic nose distinguishes exhaled breath of patients with malignant pleural mesothelioma from controls." *Lung Cancer*, **75**, 326 (2012).
284. S. Dragonieri, J. T. Annema, R. Schot, M. P. van der Schee, A. Spanevello, P. Carratù, O. Resta, K. F. Rabe, and P. J. Sterk, "An electronic nose in the discrimination of patients with non-small cell lung cancer and COPD." *Lung Cancer*, **64**, 166 (2009).
285. Z. Q. Xu et al., "A nanomaterial-based breath test for distinguishing gastric cancer from benign gastric conditions." *Br. J. Cancer*, **108**, 941 (2012).
286. C. Timms, P. S. Thomas, and D. H. Yates, "Detection of gastro-oesophageal reflux disease (GORD) in patients with obstructive lung disease using exhaled breath profiling." *J. Breath Res.*, **6**, 016003 (2012).
287. R. Ionescu et al., "Detection of multiple sclerosis from exhaled breath using bilayers of polycyclic aromatic hydrocarbons and single-wall carbon nanotubes." *ACS Chem. Neurosci.*, **2**, 687 (2011).
288. U. Tisch et al., "Detection of Alzheimer's and Parkinson's disease from exhaled breath using nanomaterial-based sensors." *Nanomedicine (Lond.)*, **8**, 43 (2013).
289. G. Shuster et al., "Classification of breast cancer precursors through exhaled breath." *Breast Cancer Res. Treat.*, **126**, 791 (2011).
290. Z. Lazar, N. Fens, J. van der Maten, M. P. van der Schee, A. H. Wagener, S. B. de Nijs, E. Dijkers, and P. J. Sterk, "Electronic nose breathprints are independent of acute changes in airway caliber in asthma." *Sensors*, **10**, 9127 (2010).
291. N. Fens, R. A. Douma, P. J. Sterk, and P. W. Kamphuisen, "Breathomics as a diagnostic tool for pulmonary embolism." *J. Thromb. Haemost.*, **8**, 2831 (2010).
292. E. A. Chapman, P. S. Thomas, E. Stone, C. Lewis, and D. H. Yates, "A breath test for malignant mesothelioma using an electronic nose." *Eur. Respir. J.*, **40**, 448 (2012).
293. H. Biller, O. Holz, H. Windt, W. Koch, M. Müller, R. A. Jörres, N. Krug, and J. M. Hohlfeld, "Breath profiles by electronic nose correlate with systemic markers but not ozone response." *Respir. Med.*, **105**, 1352 (2011).
294. A. H. Jalal, Y. Umasankar, F. Christopher, E. A. Pretto Jr, and S. Bhansali, "A model for safe transport of critical patients in unmanned drones with a 'watch' style continuous anesthesia sensor." *J. Electrochem. Soc.*, **165**, B3071 (2018).
295. J. Ozhikandathil, S. Badilescu, and M. Packirisamy, "Polymer composite optically integrated lab on chip for the detection of ammonia." *J. Electrochem. Soc.*, **165**, B3078 (2018).
296. Y. Chung, H. Park, E. Lee, S.-H. Kim, and D.-J. Kim, "Communication—gas sensing behaviors of electrophoretically deposited nickel oxide films from morphologically tailored particles." *J. Electrochem. Soc.*, **163**, B624 (2016).
297. S. Ozdemir, T. B. Osburn, and J. L. Gole, "Nanostructure modified gas sensor detection matrix for NO transient conversion of NO to NO<sub>2</sub>." *J. Electrochem. Soc.*, **158**, J201 (2011).

298. N. Shehada, G. Brönstrup, K. Funka, S. Christiansen, M. Leja, and H. Haick, "Ultrasensitive silicon nanowire for real-world gas sensing: noninvasive diagnosis of cancer from breath volatolome." *Nano Lett.*, **15**, 1288 (2014).
299. K.-W. Kao, M.-C. Hsu, Y.-H. Chang, S. Gwo, and J. A. Yeh, "A sub-ppm acetone gas sensor for diabetes detection using 10 nm thick ultrathin InN FETs." *Sensors (Basel)*, **12**, 7157 (2012).
300. P. J. Mazzone, X. F. Wang, Y. Xu, T. Mekhail, M. C. Beukemann, J. Na, J. W. Kemling, K. S. Suslick, and M. Sasidhar, "Exhaled breath analysis with a colorimetric sensor array for the identification and characterization of lung cancer." *J. Thorac. Oncol.*, **7**, 137 (2012).
301. P. J. Mazzone, J. Hammel, R. Dweik, J. Na, C. Czich, D. Laskowski, and T. Mekhail, "Diagnosis of lung cancer by the analysis of exhaled breath with a colorimetric sensor array." *Thorax*, **62**, 565 (2007).
302. N. Alagirisamy, S. S. Hardas, and S. Jayaraman, "Novel colorimetric sensor for oral malodour." *Anal. Chim. Acta*, **661**, 97 (2010).
303. A. D'Amico, G. Penazza, M. Santonico, E. Martinelli, C. Roscioni, G. Galluccio, R. Paolesse, and C. Di Natale, "An investigation on electronic nose diagnosis of lung cancer." *Lung Cancer*, **68**, 170 (2010).
304. C. Di Natale, A. Macagnano, E. E. Martinelli, R. Paolesse, G. D'Arcangelo, C. Roscioni, A. Finazzi-Agro, and A. D'Amico, "Lung cancer identification by the analysis of breath by means of an array of non-selective gas sensors." *Biosens. Bioelectron.*, **18**, 1209 (2003).
305. R. A. Incalzi, G. Pennazza, S. Scarlata, M. Santonico, M. Petriaggi, D. Chirurgo, C. Pedone, and A. D'Amico, "Reproducibility and respiratory function correlates of exhaled breath fingerprint in chronic obstructive pulmonary disease." *PLoS One*, **7**, e45396 (2012).
306. P. Montuschi, M. Santonico, C. Mondino, G. Pennazza, G. Mantini, E. Martinelli, R. Capuano, G. Ciabattini, R. Paolesse, C. Di Natale, P. J. Barnes, and A. D'Amico, "Diagnostic performance of an electronic nose, fractional exhaled nitric oxide, and lung function testing in asthma." *Chest*, **137**, 790 (2010).
307. G. Pennazza, E. Marchetti, M. Santonico, G. Mantini, S. Mummolo, G. Marzo, R. Paolesse, A. D'Amico, and C. Di Natale, "Application of a quartz microbalance based gas sensor array for the study of halitosis." *J. Breath Res.*, **2**, 017009 (2008).
308. X. Chen, M. Cao, Y. Li, W. Hu, P. Wang, K. Ying, and H. Pan, "A study of an electronic nose for detection of lung cancer based on a virtual SAW gas sensors array and imaging recognition method." *Meas. Sci. Technol.*, **16**, 1535 (2005).
309. M. Phillips et al., "Point-of-care breath test for biomarkers of active pulmonary tuberculosis." *Tuberculosis*, **92**, 314 (2012).
310. M. S. Cristescu, J. Mandon, M. J. F. Harren, P. Merilainen, and M. H. Ogman, "Methods of NO detection in exhaled breath." *J. Breath Res.*, **7**, 017104 (2013).
311. W.-K. Jo and K.-B. Song, "Exposure to volatile organic compounds for individuals with occupations associated with potential exposure to motor vehicle exhaust and/or gasoline vapor emissions." *Sci. Total Environ.*, **269**, 25 (2001).
312. F. Brugnone, L. Perbellini, G. B. Faccini, F. Pasini, B. Danzi, G. Maranelli, L. Romeo, M. Gobbi, and A. A. Zedde, "Benzene in the blood and breath of normal people and occupationally exposed workers." *Am. J. Ind. Med.*, **16**, 385 (1989).
313. T. Wang, A. Pysanenko, K. Dryahina, and P. Španěl, "Analysis of breath, exhaled via the mouth and nose, and the air in the oral cavity." *J. Breath Res.*, **2**, 037013 (2008).
314. J. Taucher, A. Hansel, A. Jordan, R. Fall, J. H. Futrell, and W. Lindinger, "Detection of isoprene in expired air from human subjects using proton-transfer-reaction mass spectrometry." *Rapid. Commun. Mass Spectrom.*, **11**, 1230 (1997).
315. D. Smith, P. Španěl, B. Enderby, W. Lenney, C. Turner, and S. J. Davies, "Isoprene levels in the exhaled breath of 200 healthy pupils within the age range 7–18 years studied using SIFT-MS." *J. Breath Res.*, **4**, 017101 (2010).
316. M. Lechner, B. Moser, D. Niederseer, A. Karlseder, B. Holzknacht, M. Fuchs, S. Colvin, H. Tilg, and J. Rieder, "Gender and age specific differences in exhaled isoprene levels." *J. Respir. Physiol. Neurobiol.*, **154**, 478 (2006).